# The geometry of coexistence in large ecosystems

Jacopo Grilli,[1,*] Matteo Adorisio,[2] Samir Suweis,[2] Gyuri Barabás,[1]

Jayanth R. Banavar,[3] Stefano Allesina,[1,4,†] and Amos Maritan[2,‡]

[1]*Dept. of Ecology & Evolution, University of Chicago. Chicago, IL 60637, USA*

[2]*Dept. of Physics and Astronomy "Galileo Galilei", Università degli Studi di Padova, Padova, Italy*

[3]*Department of Physics, University of Maryland, College Park, MD 20742, USA*

[4]*Computation Institute, University of Chicago*

The role of interactions in shaping the interplay between the stability of an ecosystem and its biodiversity is still not well understood. We introduce a geometrical approach, that lends itself to both analytic and numerical analyses, for studying the domain of interaction parameters that results in stable coexistence. We find the remarkable result that just a few attributes of the interactions are responsible for stable coexistence in large random ecosystems. We analyze more than 100 empirical networks and find that their architecture generally has a limited effect on in sustaining biodiversity.

Natural populations are faced with constantly varying environmental conditions. Because environmental conditions affect physiological parameters (e.g., metabolic rates [1]) as well as ecological ones (e.g., the presence and strength of interactions between populations [2–5]), in order to persist ecological communities necessarily need at least to be able to cope with small changes in environmental conditions. Mathematically, this translates into an argument on the robustness of the qualitative behavior of an ecological dynamical system: to guarantee robust coexistence, a model describing an ecological community needs at least to be (qualitatively) insensitive to small perturbations of the parameters. This notion has been formalized in the measure of "structural stability" [6], expressed as the "volume" of the parameter space resulting the coexistence of all populations in an ecological community.

While local asymptotic stability (i.e., the ability to recover after a small changes in the densities of the population abundances) of ecological communities has been studied in small [7] and large [8–10] systems, the study of structural stability (i.e., the ability of a community to persist if conditions are slightly altered)—despite being proposed early on as a key characteristic in the context of the diversity-stability debate [11–13]—has historically been restricted to the case of small communities, with the first studies of larger communities appearing only recently [14], and—because of mathematical limitations—dealing exclusively with the case of large mutualistic communities. Studies of structural stability have so far focused on the effect of ecological network structure (who interacts with whom) on the volume of parameter space leading to "feasible" equilibria, in which all populations have positive densities.

---

[*]Electronic address: jgrilli@uchicago.edu

[†]Electronic address: sallesina@uchicago.edu

[‡]Electronic address: maritan@pd.infn.it

Here we develop a geometrical framework for studying the feasibility of large ecological communities. We overcome the limitations that have hitherto prevented the study of consumer-resource networks thereby providing a unified view of feasibility in ecological systems. Using a random matrix approach (which helped in identifying the main drivers of local asymptotic stability), we pinpoint the key quantities that control the volume of feasible parameters, as well as the sensitivity to changes in these parameters. We then contrast these expectations for randomly connected systems with simulations on structured empirical networks and demonstrate that network structure has limited effects on feasibility.

For simplicity, we consider a community composed of $S$ populations, whose dynamics are determined by a system of autonomous ODEs:

$$\frac{dn_i}{dt} = r_i n_i + n_i \sum_{j=1}^{S} A_{ij} n_j \ , \tag{1}$$

where $n_i$ is the density of population $i$, $r_i$ is its intrinsic growth rate, and $A_{ij}$ (which in principle could depend on $\mathbf{n}$, Supplementary Information) measures the interaction strength between population $i$ and $j$. A fixed point $n_i^*$ (i.e., a vector of densities making the right side of each equation zero) is feasible if $n_i^* > 0$ for every population. A fixed point is locally stable if, following any (small enough) perturbation of the densities, the system returns to the fixed point. The fixed point is globally stable if the system eventually reaches it starting from any feasible initial condition. A system is structurally stable if, following a change of the growth rates $\mathbf{r}$, the new fixed point is still stable and feasible.

To study the range of conditions leading to stable coexistence, we need to disentangle feasibility and local stability. This problem is well discussed in Rohr *et al.* [14], where it was solved for the case of a possible parametrization of mutualistic interactions. In the Supplementary Information, we obtain a criterion for the matrix $\mathbf{A}$, which is valid irrespective of the parametrization. In particular, we show that if all the eigenvalues of $\mathbf{A} + \mathbf{A}^t$ are negative (i.e., the matrix $\mathbf{A}$ is non-reactive [15]), then global stability holds for any feasible fixed point. Using this criterion, we can extend the study of feasibility to food webs and other ecological networks.

We want to measure the space of growth rates $\mathbf{r}$ leading to the coexistence of all $S$ populations. Since we can separate stability and feasibility, we only need to find the space of $\mathbf{r}$ leading to feasible fixed points, and the criterion above ensures that these will be globally stable. As pointed out before [14], the problem is not to find a particular parameterization $\mathbf{r}$ leading to coexistence, but rather to measure how flexibly, we may choose these rates. As shown in Fig. 1, this quantity—indicated by $\Xi$ henceforth—, can be thought as a volume, or more precisely a solid angle, in the space of growth rates.

To calculate $\Xi$, one might naively wish to numerically compute directly the proportion of growth rates leading to a feasible equilibrium. While a direct calculation is viable when $S$ is small enough, this procedure becomes extremely inefficient for large $S$ [14]. Previous approaches have therefore relied on indirect quantifications of this space [14, 16], so that, rather than calculating $\Xi$ directly, one might correlate it with properties of interest. In the Supplementary

Information we introduce a method, based on a change of variables, that can be used to calculate $\Xi$ with arbitrary precision. Using this method, we can measure accurately the size of the coexistence domain, with larger values of $\Xi$ corresponding to larger proportions of conditions (intrinsic growth rates) compatible with stable coexistence. For reference, we normalize $\Xi$ so that $\Xi = 1$ when populations are not interacting (Supplementary Information), i.e., when all the off-diagonal elements of the interaction matrix $\mathbf{A}$ are equal to zero, and thus Eq. 1 simplifies to $S$ independent logistic equations.

Since May's seminal work [8], random matrices have been a reference null model for ecological interactions. A particularly interesting feature of random matrices is that their spectrum (i.e., the distribution of their eigenvalues, which determines local stability), is *universal* [17]. This means that local stability depends on just a few, coarse-grained properties of the matrix (e.g., the first two moments of the distribution of interaction strengths) and not on the finer details (e.g., the particular distribution of interaction strengths, see Supplementary Information). Surprisingly, we find that the feasibility of random matrices is also universal (Supplementary Information): $\Xi$ depends only on the connectance (the probability of interaction), and the first few moments of the distribution of interaction strengths. These moments can be combined into three parameters, $E_1$, $E_2$ and $E_c$ * which, together with $S$, completely determine the size of the feasibility domain $\Xi$ (see Supplementary Information). Two very different (random) ecosystems, with different interaction types and different distributions of interaction strengths, but having the same number of populations and the same $E_1$, $E_2$ and $E_c$, have the same $\Xi$ in the large $S$ limit. This result has important theoretical implications, but also very practical consequences, namely that the parameter space one needs to explore is dramatically reduced.

Using the numerical method explained in the Supplementary Information, we find that, when the mean and variance of interaction strengths when not too large (Supplementary Information), for random interaction matrices $A$,

---

* $E_1$, $E_2$ and $E_c$ are moments of the interaction matrix and are simply and directly related with the interaction strenghts. They are defined as

$$E_1 = \frac{1}{S(S-1)} \sum_{i \neq j} M_{ij}$$

$$E_2^2 = \frac{1}{S(S-1)} \sum_{i \neq j} M_{ij}^2 - E_1^2 \tag{2}$$

$$E_c = \frac{1}{S(S-1)E_2^2} \sum_{i \neq j} M_{ij} M_{ji} - \frac{E_1^2}{E_2^2} \ .$$

In the case of a random network with connectance $C$ they reduces to [17]

$$E_1 = C\mu$$

$$E_2^2 = C(1-C)\mu^2 + C\sigma^2 \tag{3}$$

$$E_c = \frac{\rho\sigma^2 + (1-C)\mu^2}{\sigma^2 + (1-C)\mu^2} \ ,$$

where $\mu$ is the mean of the interaction strenghts, $\sigma$ is the variance and $\rho$ is the correlation between the interaction strenghts of pairs of species interacting togheter [17].

$$\Xi \sim \left(1 - \frac{1}{\pi}\frac{E_1(SE_1 - 2d)}{\pi(d - SE_1^2)}\right)^{-S}, \tag{4}$$

where $S$ is is the number of populations, $d$ is the mean of the diagonal entries of $A$, and $E_1 = C\mu$, where $C$ is the connectance and $\mu$ is the average interaction strength. In the Supplementary Information a more accurate prediction is presented.

Given that $d$ is negative by definition (SI), depending on the sign of $\mu$, having more species can either increase ($\mu > 0$) or shrink ($\mu < 0$) the size of feasibility domain. It is important to stress that, since we have disentangled feasibility and stability, we can compute $\Xi$ without considering stability, but coexistence depends on both. When we consider how $\Xi$ depends on $S$ and other parameters, we need to take into account what the conditions are that make the matrix non-reactive (see Supplementary Information). In the case of positive interaction strengths, this condition is $d + SC\mu < 0$, implying an upper bound for $\mu$ that depends on $S$.

Having explored the feasibility of random networks, we proceed to investigate the effects of incorporating empirical network structure. Ecological networks, in fact, are not random [18–20], and many studies have hypothesized that the structure of interactions could increase the likelihood of coexistence of distinct species [21–23]. Because we can calculate $\Xi$ for any $A$, we can directly compare the domain of coexistence of empirical networks to their random counterparts. In this way, we can explicitly test whether empirical topologies are more conducive to feasibility. Fig. 2 shows the values of $\Xi$ for 89 mutualistic networks and 15 food-webs (Supplementary Information). Contrary to expectations [14], we find that empirical mutualistic networks have values of $\Xi$ that are more or less indistinguishable from those of their corresponding randomizations. While our results suggest that mutualistic network structure has little impact on feasibility, we find that food web structure does affect the size of the domain of coexistence, but in a negative way: empirical interaction structures have lower values of $\Xi$ compared to their randomized counterparts.

Until now, we have concentrated on the volume of the parameter space resulting in feasiblity. However, two systems having the same $\Xi$ can yet have very different responses to perturbations in the interaction parameters, just as two triangles having the same area need not have sides of the same length (Fig. 1). The two extreme cases correspond to a) an isotopic system in which, if we start at the baricenter of the feasibility domain, moving in any direction yields roughly the same effect (equivalent to an equilateral triangle), b) anisotropic systems in which certain directions are more dangerous than others (as in a scalene triangle). For our problem, the domain of growth rates leading to coexistence is—once the growth rates are normalized—the $(S-1)$-dimensional generalization of a triangle on a hypersphere. When $S = 3$ this domain is indeed a triangle lying on a sphere as shown in Fig. 1. If all the $S(S-1)/2$ sides of this (hyper-)triangle are about the same length, then different perturbations will have similar effects on the system. On the other hand, if some sides are much shorter than others, then there will be changes of conditions which will more likely impact coexistence than others. We therefore consider a measure of the heterogeneity in the distribution of the lengths of the sides (Fig. 1 and Supplementary Information). The broader the distribution

(e.g., the larger its variance), the more heterogeneous the response to perturbations will be. This way of measuring heterogeneity is particularly convenient, because it is independent of the initial conditions. Moreover, the length of each side can be directly related to the similarity between the corresponding pair of species (see Supplementary Information), drawing a strong connection between the space of coexistence and the phenotypic space. As in the case of $\Xi$, this measure is a function of the interaction matrix and corresponds to a geometrical property of the coexistence domain.

While $\Xi$ is a universal quantity for random networks, the distribution of side lengths is not (Supplementary Information)—it depends on the full distribution of interaction strengths. Despite this fact, it is possible to compute it analytically in full generality (Supplementary Information) and obtain an expression for its mean and variance, which depend only on $S$, $E_1$, $E_2$ and $E_c$ (Supplementary Information). Fig. 3 shows that the analytical formula, in the case of random $A$, matches the observed mean and the variance of sides lengths perfectly.

As we have done for $\Xi$, we can now test how non-random empirical network topologies influence the distribution of sides lengths. We tested this effect for four types of structures: bipartite, cascade [18], modular, and perfectly nested topologies. (Fig. 3 and Supplementary Information). All these structures have modest effects on the mean side length. The effect on the variance of side lengths is more pronounced, with a modular structure significantly increasing the variance. Fig. 3 demonstrates that empirical food webs have smaller side lengths and higher variances. This is consistent with the low values of $\Xi$ displayed in Fig. 1. For mutualistic networks, the mean side lengths coincide with those expected for the random counterparts whereas the variances are much larger than those expected by chance. This indicates that empirical mutualistic networks are characterized by some directions of perturbations that are more dangerous than others.

Several studies investigated the effect of network structure on species coexistence [21–24]. Here we have shown that the proportion of conditions compatible with coexistence is mainly determined by the number and strength of interactions. In terms of network properties, the relevant quantity is connectance, with other properties (e.g., nestedness or degree distribution) having minimal effects. In particular, once the connectance and mean interaction strength are fixed, matrices built using empirical mutualistic networks have $\Xi$ that is not much different from that expected for a random case, as observed in a similar context [25]. Empirical food webs, on the other hand, tend to have $\Xi$ smaller than their random counterparts. These results parallel those for the distribution of side lengths: while the mean side length for an empirical structure is similar to that of the corresponding random web, the variance is much higher, implying that for some directions, even small perturbations of the parameters could drive the system outside its feasibility domain.
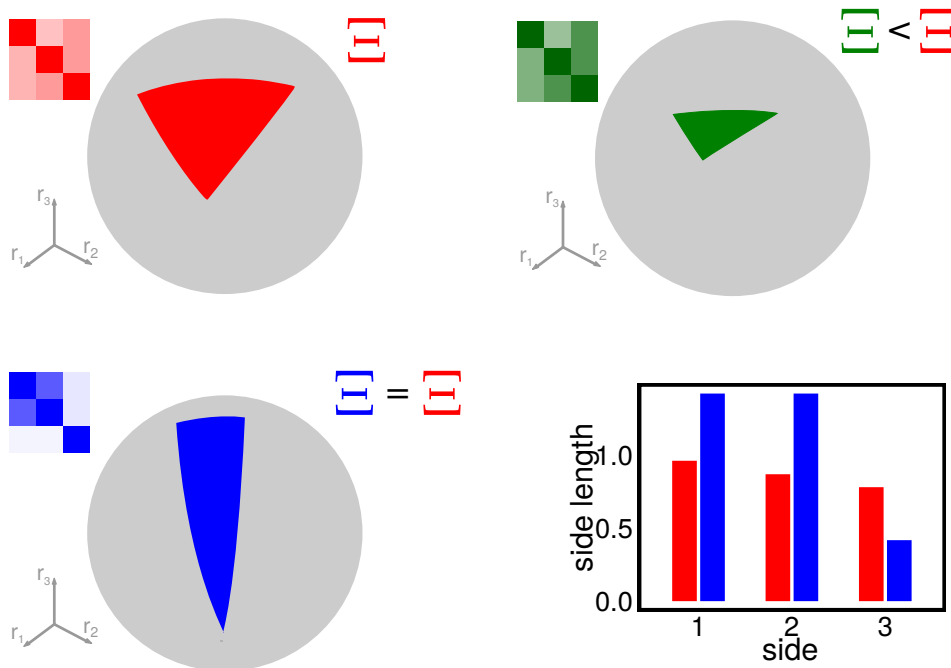
FIG. 1: **Geometrical properties of feasibility.** The panels show the size and shape of the feasibility domain for three interaction matrices, each defining the interactions among three populations. If $\mathbf{r}$ corresponds to a feasible equilibrium, also $c\mathbf{r}$ does, for any positive $c$. We can therefore study the feasibility domain on the surface of a sphere (see Supplementary Information). The gray sphere represents the $S = 3$-dimensional space of growth rates, while the colored part correspond to the combination of growth rates leading to stable coexistence. The area (or volume for higher-dimensional systems) of the colored part is measured by $\Xi$. Larger values of $\Xi$ correspond to a higher proportion of combinations of growth rates leading to coexistence (i.e., more "structurally stable"): the red interaction matrix is more structurally stable than the green one. The size of this region (i.e., the value of $\Xi$) does not capture all the properties relevant for coexistence. The red and blue systems have the same $\Xi$, but the two regions—despite having the same area—have very different shapes, summarized in the bottom-right panel, where we show the length of each side for the red and blue systems. In the red system, the three sides have about the same length, and thus moving from the center in any direction will have about the same effect; in the blue system, one side is much shorter than the other two, implying that for some specific direction, even small perturbations could drive the system outside the feasibility domain.
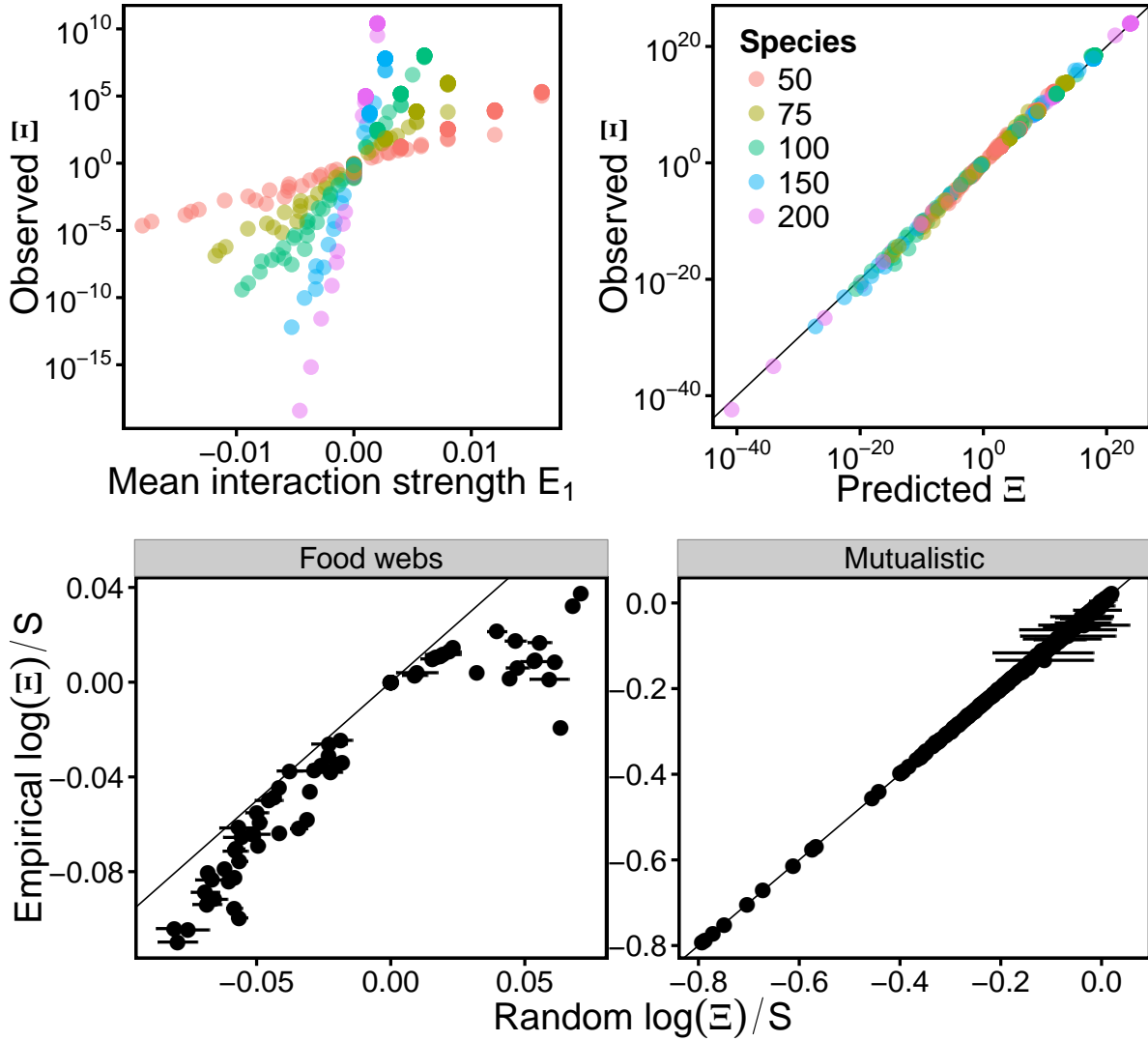
FIG. 2: **Domain of coexistence in random and empirical webs.** The top two panels show $\Xi$, the size of the domain of growth rates leading to coexistence, in the case of random networks. The left panel shows the dependence of $\Xi$ on $E_1 = C\mu$ (where $C$ is the connectance and $\mu$ is the mean interaction strength), and number of species $S$. The right panel shows the match between our analytical prediction (Eq. 4 and Supplementary Information) and the numerical determined value of $\Xi$. The bottom panels show a comparison between $\Xi$ computed for empirical webs (89 mutualistic networks on the right, and 15 food-webs on the left) and that computed for their random counterparts (Supplementary Information). Each network was parametrized with different distributions of interaction strengths (Supplementary Information). Mutualistic networks have values of $\Xi$ comparable with the corresponding randomizations, indicating that their structure does not influence the size of the domain of coexistence. Food webs have lower values of $\Xi$ than their random counterparts. Empirical networks were parametrized extracting interaction strengths from a bivariate normal distribution with different means, variances and correlations (see Supplementary Information).
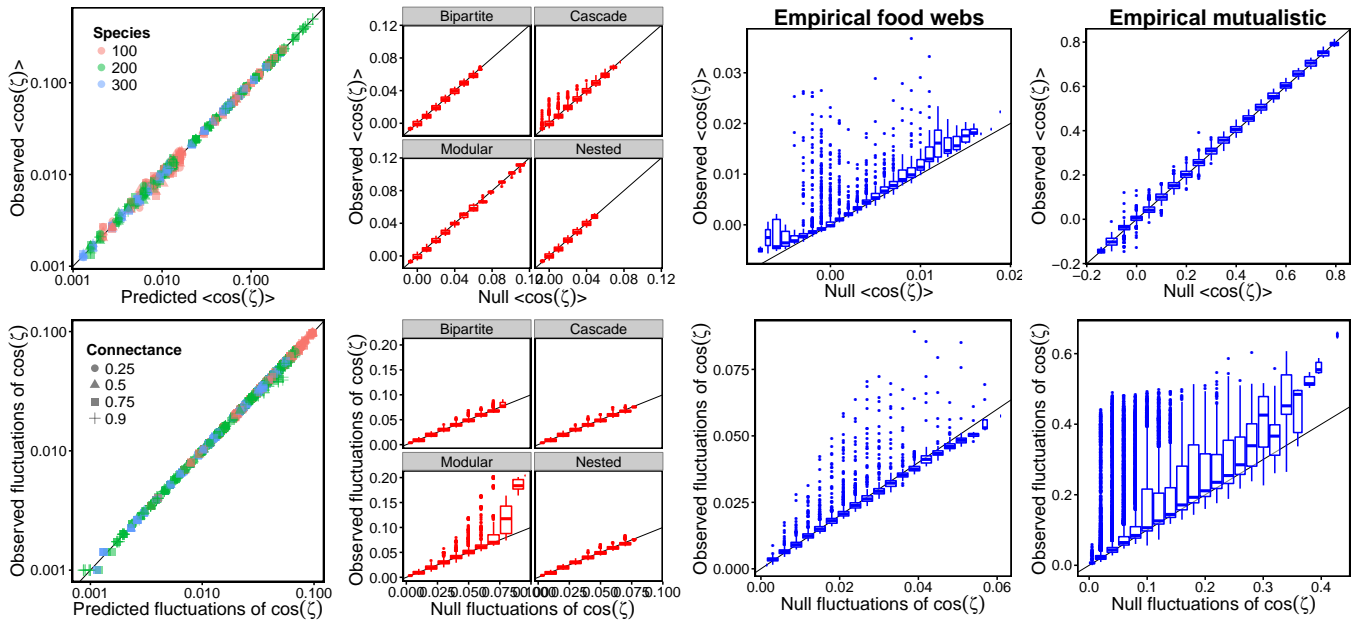
FIG. 3: **Distribution of side lengths in random, structured and empirical networks.** Left panels show the mean and the standard deviation of $\cos(\eta)$, where $\eta$ is the side length. Analytical predictions for the first two moments of $\cos(\eta)$ (Supplementary Information) perfectly match the numerical simulations. The panels in the middle show the effect of non-random structure on the first two moments of $\cos(\eta)$. Largest values of the mean $\langle \cos(\eta) \rangle$ (corresponding to smaller side lengths) are present only in the case of the cascade model. Strong fluctuations in $\cos(\eta)$ (and therefore in side lengths) are visible in the case of modular structure. The four panels on the right show mean and standard deviation of $\cos(\eta)$ for mutualistic and food webs compared to the expectations for the randomized cases. While food webs display smaller mean side lengths (consistent with the small $\Xi$ observed in Fig. 2), both trophic and mutualistic interactions show larger fluctuations of side lengths, suggesting the existence of perturbation directions that are more dangerous than others.

# The geometry of coexistence in large ecosystems
# Supplementary Information

## Contents

## S1. COMMUNITY DYNAMICS, FEASIBILITY, AND STABILITY

We consider an ecological community composed of $S$ populations, whose growth rates are described by the following equations:

$$\frac{\mathrm{d}n_i}{\mathrm{d}t} = n_i \left( r_i + \sum_{j=1}^{S} A_{ij} n_j \right) , \tag{S1}$$

where $n_i$ is the population abundance of species $i$ and $r_i$ is its intrinsic growth rate, and $A_{ij}$ is the effect of a unit change in species $j$'s density on species $i$'s per capita growth rate. For notational convenience, we collect the coefficients $A_{ij}$ into the interaction matrix $\mathbf{A}$, and $n_i$ and $r_i$ into the vectors $\mathbf{n}$ and $\mathbf{r}$, respectively.

In principle, the interaction matrix $\mathbf{A}$ may depend on $\mathbf{n}$. We discuss this more general case in section S12. In the following, we consider the simpler case of $\mathbf{A}$ being independent of $\mathbf{n}$; then, equation (S1) is a system of generalized Lotka–Volterra equations.

A vector $\mathbf{n}^*$ is a fixed point (equilibrium) if

$$0 = n_i^* \left( r_i + \sum_{j=1}^{S} A_{ij} n_j^* \right) \qquad (i = 1, 2, \ldots, S) . \tag{S2}$$

A fixed point is feasible if $n_i^* > 0$ for all $i$. A feasible fixed point (if it exists) is then a solution to the equation

$$r_i = -\sum_{j=1}^{S} A_{ij} n_j^* , \tag{S3}$$

and therefore, assuming $\mathbf{A}$ is invertible,

$$n_i^* = -\sum_{j=1}^{S} A_{ij}^{-1} r_j . \tag{S4}$$

A fixed point $n_i^*$ is locally stable if the system returns to it following any sufficiently small perturbation of the population abundances. Introducing $n_i = n_i^* + \delta n_i$ in equation S1 and assuming that $\delta n_i$ is small, we obtain, by expanding around $\delta n_i = 0$,

$$\frac{\mathrm{d}\delta n_i}{\mathrm{d}t} = \sum_{j=1}^{S} M_{ij} \delta n_j , \tag{S5}$$

where $\mathbf{M}$ is the Jacobian evaluated at the fixed point (also called the community matrix), which, in the case of equation S1, reduces to

$$M_{ij} = n_i^* A_{ij} = -\left( \sum_{k=1}^{S} A_{ik}^{-1} r_k \right) A_{ij} . \tag{S6}$$

Substituting into equation S5, we get

$$\frac{\mathrm{d}\delta n_i}{\mathrm{d}t} = -\sum_{j=1}^{S} \left( \sum_{k=1}^{S} A_{ik}^{-1} r_k \right) A_{ij} \delta n_j . \tag{S7}$$

There are two possible scenarios for the dynamics of equation S5. If all eigenvalues of $\mathbf{M}$ have negative real parts, then the perturbation $\delta \mathbf{n}$ decays exponentially to zero and $n_i^*$ is locally stable. If at least one eigenvalue of $\mathbf{M}$ has a positive real part, then there exists an infinitesimal perturbation such that the system does not return to equilibrium. If we order the eigenvalues $\lambda_i$ of $\mathbf{M}$ according to their real parts, i.e., $\Re(\lambda_1) > \Re(\lambda_2) > \cdots > \Re(\lambda_S)$, then stability depends exclusively on $\Re(\lambda_1)$: if it is negative, $n_i^*$ is dynamically locally stable; otherwise, it is unstable.

A fixed point is globally stable if it is the final outcome of the dynamics from any initial condition involving strictly positive population abundances.

## S2.   DISENTANGLING STABILITY AND FEASIBILITY

As we can see from equations S4 and S7, both feasibility and stability depend on both $\mathbf{r}$ and $\mathbf{A}$ and, at least in principle, a fixed point can be stable or unstable, independently of the fact that it is feasible or not.

We want to study the proportion of conditions (i.e., the number of combinations of the growth rates $\mathbf{r}$ out of all possible combinations) leading to coexistence, i.e., leading to stable and feasible equilibria. Therefore in principle we should, for a fixed matrix $\mathbf{A}$, look for growth rates $\mathbf{r}$ that satisfy both stability and feasibility. In probabilistic terms, we want to measure the likelihood that a random combination of the intrinsic growth rates corresponds to a stable and feasible solution.

In the case of equation S1, it is possible to disentangle feasibility and stability by applying a mild condition on the interaction matrix $\mathbf{A}$. To this end, we introduce some terminology [26, section 2.1.2]:

- **Stability**. A real matrix $\mathbf{B}$ is stable if all its eigenvalues have negative real parts.

- **D-stability**. A real matrix $\mathbf{B}$ is D-stable if $\mathbf{D}\,\mathbf{B}$ is stable for any diagonal matrix $\mathbf{D}$ with strictly positive diagonal entries.

- **Diagonal stability**. A real matrix $\mathbf{B}$ is diagonally stable if there exists a positive diagonal matrix $\mathbf{D}$ such that $\mathbf{D}\,\mathbf{B} + \mathbf{B}^t\,\mathbf{D}$ is stable (where $\mathbf{B}^t$ is the transpose of $\mathbf{B}$).

- **Reactivity**. A real matrix $\mathbf{B}$ is reactive if $\mathbf{B} + \mathbf{B}^t$ is unstable.

These properties are closely related to each other [26, 27]:

$$\text{Nonreactivity} \implies \text{Diagonal stability} \implies \text{D-stability} \implies \text{Stability} \tag{S8}$$

- **Nonreactivity $\implies$ Diagonal stability**. If a matrix is not reactive, then the positive diagonal matrix satisfying the condition for diagonal stability is simply the identity matrix.

- **Diagonal stability $\implies$ D-stability**. See the book by Kaszkurewicz & Bhaya for the proof [26, lemma 2.1.4].

- **D-Stability $\implies$ Stability**. This follows from the definition of D-stability when $\mathbf{D}$ is the identity matrix.

In the case of equation S1, those conditions applied to the matrix $\mathbf{A}$ are related to the stability of the system. One can use the definition of the community matrix (equation S6) to show that **D-Stability of A implies the local asymptotic stability of *any* feasible fixed point**. This is because the community matrix $M_{ij} = n_i^* A_{ij}$ can be written as $\mathbf{N} \mathbf{A}$, where $\mathbf{N}$ is a diagonal matrix with $N_{ii} = n_i^*$. If the fixed point is feasible and $\mathbf{A}$ is D-stable, then local asymptotic stability is guaranteed. Moreover it is possible to show [14, 28] that **diagonal stability of A $\implies$ global stability**.

Thus, we have a condition on $\mathbf{A}$ that makes it possible to disentangle the problems of stability and feasibility: **A is nonreactive $\implies$ global stability of the feasible fixed point**. Therefore, if we assume $\mathbf{A}$ is nonreactive, then feasibility of the equilibrium is sufficient to guarantee its global stability as well, i.e., feasibility guarantees globally stable coexistence. Consistently with this, it is known that the largest eigenvalue of $(\mathbf{A} + \mathbf{A}^t)/2$ is always larger than or equal to the real part of $\mathbf{A}$'s leading eigenvalue [15], implying that reactivity always precedes instability (or that nonreactivity implies stability). While this was indeed observed before, it is important to underline that, in the case of ref. [15], this property was considered on the community matrix $\mathbf{M}$ (which also depends on the fixed point's position in phase space) and not on the interaction matrix $\mathbf{A}$.

Since we are interested in studying how interactions (i.e., the matrix $\mathbf{A}$) determine coexistence, and which properties of the former determine the latter, we will restrict our analysis to nonreactive matrices $\mathbf{A}$ and focus only on the problem of feasibility. This criterion has the advantage of being analytically computable for large random matrices (see section S5 A).

## S3. GEOMETRICAL PROPERTIES OF THE FEASIBILITY DOMAIN

In section S2 we showed how to separate feasibility and stability, i.e., we have a criterion on the interaction matrix that guarantees (global) stability of the feasible fixed point. The problem of determining the size of the coexistence domain is therefore reduced to that of determining the size of the feasibility domain. The ecological interpretation of this volume is the proportion of different conditions leading to feasible equilibria out of all possible conditions. The larger this volume is, the higher the probability that the system is able to sustain biodiversity. In terms of equation S1, we want to quantify the proportion of growth rate vectors $\mathbf{r}$ corresponding to a feasible fixed point.

At this point, it is important to observe that if a vector $\mathbf{r}$ corresponds to a feasible solution, then $c\mathbf{r}$, $c$ being an arbitrary positive constant, also corresponds to a feasible solution. This is because the equilibrium solution $n_i^*$ is given by equation S4, which is linear in $r_i$. Therefore, the equilibrium corresponding to $cr_i$ is simply $cn_i^*$, and since $c$ is positive, $cn_i^*$ is also feasible.

This fact implies that, given a large number of growth rate vectors $\mathbf{r}$, the expected proportion of vectors correspond-

ing to a feasible fixed point is independent of $\mathbf{r}$'s norm. In other words, $\mathbf{r}$ is feasible if and only if $\mathbf{r}/\|\mathbf{r}\|$ is feasible, where $\|\mathbf{r}\| = \sqrt{\sum_i r_i^2}$ is the Euclidean norm of $\mathbf{r}$. The proportion of feasible growth rates among all possible ones is therefore equal to the proportion of feasible growth rates calculated using only growth rate vectors with $\|\mathbf{r}\| = 1$; i.e., those lying on the unit sphere.

Before proceeding with the mathematical definition of the size of the feasibility domain, we discuss the geometrical interpretation of equation S4. From this equation, the feasibility condition reads

$$\sum_{j=1}^{S} A_{ij}^{-1} r_j < 0 . \tag{S9}$$

This equation defines a convex polyhedral cone in the $S$-dimensional space of growth rates. A convex polyhedral cone [29] is a subset of $\mathbb{R}^S$ whose elements $\mathbf{x}$ can be written as positive linear combinations of $N_G$ different $S$-dimensional vectors $\mathbf{g}^k$ called the generators of the cone:

$$\mathbf{x} = \sum_{k=1}^{N_G} \mathbf{g}^k \lambda_k , \tag{S10}$$

where the $\lambda_k$ are arbitrary positive constants. Due to this arbitrariness, if $\mathbf{g}^k$ is a generator of a given convex polyhedral cone, then also $c\mathbf{g}^k$ (where we rescale just the $k$th generator with the positive constant $c$, leaving the others unchanged) will be a generator of the *same* cone. In the case of equation S4, each and every growth rate vector belonging to the feasibility domain can be written as

$$r_i = -\sum_{k=1}^{S} A_{ik} n_k^* , \tag{S11}$$

where, by definition, $n_k^*$ is feasible and therefore a positive constant. One can easily see that this equation corresponds to equation S10 where the number of generators $N_G$ is equal to $S$ and the $i$th component of the vector $\mathbf{g}^k$ is proportional to $-A_{ik}$. As the lengths of the generators can be set to any positive value, we will normalize them to one, i.e.,

$$g_i^k(\mathbf{A}) = \frac{-A_{ik}}{\sqrt{\sum_{j=1}^{S}(A_{jk})^2}} . \tag{S12}$$

The generators completely define the feasibility domain in the space of growth rates. A growth rate vector corresponds to a feasible equilibrium if and only if it can be written as a linear combination of the generators with positive coefficients. Biologically the generators correspond to the growth rate vectors that bound the coexistence domain. They correspond to nonfeasible equilibria with just one species with positive abundance (and all the others with zero abundance), such that there exist arbitrarily small perturbations of the growth rate vector that make the equilibrium feasible.

The set of all the growth rate vectors leading to a feasible equilibrium is therefore a convex polyhedral cone, defined by

$$K(\mathbf{A}) = \{\mathbf{r} \in \mathbb{R}^S | \sum_{j=1}^{S} A_{ij}^{-1} r_j < 0\} . \tag{S13}$$

Equivalently, it can be defined in terms of the generators:

$$K(\mathbf{A}) = \{\mathbf{r} \in \mathbb{R}^S | \exists \lambda_1, \lambda_2, \ldots, \lambda_k > 0, \mathbf{r} = \sum_{k=1}^{S} \mathbf{g}^k(\mathbf{A})\lambda_k\} \, , \tag{S14}$$

where the generators $\mathbf{g}^k(\mathbf{A})$ are defined in equation S12. In section S11 we show explicitly how these concepts pan out in the case of $S = 3$.

This geometrical definition and characterization of the feasibility domain allows us to identify classes of matrices having the exact same feasibility domain: they are simply matrices having the same set of generators. In particular, there are two basic transformations of the matrix $\mathbf{A}$ (and their combinations) that leave the set of generators unchanged: permutations and positive rescaling. A square matrix $\mathbf{P}$ is a permutation matrix if each row and column has one and only one nonzero entry and the value of that entry is equal to one. A positive rescaling is performed by a positive diagonal matrix $\mathbf{D}$. The set of generators of $\mathbf{A}$ is the same as those of $\mathbf{A}\,\mathbf{P}$ and $\mathbf{A}\,\mathbf{D}$. This can be seen by observing that a permutation of the rows just changes the order of the generators but not the generators themselves. In the same way, a generator with the same direction but different length generates the same cone, and so any positive constant that rescales a row of the matrix leaves the feasibility domain unchanged. It is important to note however that these two transformations do not leave the properties of the matrix $\mathbf{A}$ unchanged: both exchanging rows of a matrix and rescaling rows by different constants will in general change the structure of the matrix.

Using this geometrical framework, one can easily identify the center of the feasibility domain (also known as structural vector [14]). There are several possible ways to define the center of a hypervolume and, without additional assumptions, all the definitions are different. One natural choice is the barycenter ("center of mass") of the domain of feasible intrinsic growth rates. Any plane passing through the barycenter divides the volume into two subvolumes of equal size. The barycenter is equivalent to the center of mass of the volume (in the case of constant density). Then, the vector $\mathbf{x}^b$ pointing from the origin to the barycenter is given by

$$\mathbf{x}^b = \int_{K(A) \cap \mathbb{S}_S} \mathrm{d}^S \mathbf{y} \ \ \mathbf{y} \, , \tag{S15}$$

where $\cap$ is the intersection of two sets, and $\mathbb{S}_S = \{\mathbf{r} \in \mathbb{R}^S | \|\mathbf{r}\| = 1\}$ represents the surface of the $S$-dimensional unit sphere. The variable $\mathbf{y}$ is therefore integrated over the feasibility domain restricted to the unit sphere's surface. All points in the feasibility domain are positive linear combinations of the generators, i.e.,

$$\mathbf{y} = \sum_k \lambda^k \mathbf{g}^k \ \ , \tag{S16}$$

where the $\lambda^k$ are positive constants. The fact that we consider only the points lying on the unit sphere, i.e., $\|\mathbf{y}\| = 1$, can be expressed as a constraint on $\lambda$ (the vector of $\lambda$s). Thus, we can write equation S15 as

$$\mathbf{x}^b = \int \mathrm{d}^S \lambda \, q(\lambda) \sum_k \lambda^k \mathbf{g}^k \, , \tag{S17}$$

where $q$ is an appropriate distribution, introduced to take into account three different constraints: all the components of $\lambda$ must be positive; the vector $\sum_k \lambda^k \mathbf{g}^k$ must lie on the unit sphere; and those vectors must be sampled uniformly on the feasibility domain. Regardless of the form of $q(\lambda)$, it is an exchangeable distribution, and therefore

$$\int d^S \lambda \, q(\lambda) \, \lambda^k = \langle \lambda \rangle \, , \tag{S18}$$

which is independent of $k$ (because the distribution $q$ is exchangeable). Therefore we obtain

$$\mathbf{x}^b = \sum_k \mathbf{g}^k \int d^S \lambda \, q(\lambda) \, \lambda^k = \sum_k \mathbf{g}^k \langle \lambda \rangle = \langle \lambda \rangle \sum_k \mathbf{g}^k \, . \tag{S19}$$

Since we want $\mathbf{x}^b$ to be normalize to one, we can fix $\langle \lambda \rangle$ using this constraint, obtaining

$$\mathbf{x}^b = \frac{1}{\sqrt{\sum_i (\sum_k g_i^k)^2}} \sum_k \mathbf{g}^k \, . \tag{S20}$$

Using equation S12, we can finally express the barycenter in terms of the matrix $\mathbf{A}$:

$$x_i^b(\mathbf{A}) = \left( \sum_i \left( \sum_k \frac{A_{ik}}{\sqrt{\sum_j (A_{jk})^2}} \right)^2 \right)^{-1/2} \sum_{k=1}^S \frac{-A_{ik}}{\sqrt{\sum_{j=1}^S (A_{jk})^2}} \, . \tag{S21}$$

## S4. DEFINITION AND CALCULATION OF Ξ

As explained in section S3, the proportion of feasible growth rates can be calculated considering only growth rate vectors of length one, i.e., $\|\mathbf{r}\| = 1$. This proportion can be interpreted as the volume of the intersection of a convex cone and the surface of a sphere. Equivalently, it is the solid angle of the convex polyhedral cone [30].

We define the quantity $\Xi$ as

$$\Xi = 2^S \frac{\text{\# growth rate vectors corresponding to a feasible fixed point}}{\text{total \# growth rate vectors}} \, . \tag{S22}$$

The factor $2^S$ that appears in this equation is an arbitrary choice, and it has been introduced to have $\Xi = 1$ when species are not interacting ($A_{ij} = 0$ if $i \neq j$). In this case equation S1 reduces to $S$ independent logistic equations with equilibrium densities $n_i^* = -r_i/A_{ii}$. Taking each $A_{ii}$ to be negative (otherwise each species would have an unstoppable positive feedback on itself), this equilibrium is feasible if and only if each $r_i$ is positive. For a single species then, the probability of randomly drawing a feasible (i.e., positive) growth rate out of all possible growth rates is one half. For two species, both growth rates must have the correct sign to have the two species with positive abundance, and therefore the proportion of growth rate vectors satisfying this condition is $1/4$. For $S$ species the combinations of the growth rates leading to a feasible fixed point is $2^{-S}$. $\Xi$, defined as in equation S22, is therefore equal to one when species do not interact.

In terms of geometrical properties and the convex polyhedral cone, $\Xi$ can be defined as

$$\Xi = 2^S \frac{\text{vol}_{S-1}(K(A) \cap \mathbb{S}_S)}{\text{vol}_{S-1}(\mathbb{S}_S)} \, , \tag{S23}$$

where $K(A)$ is defined in equation S13, $\mathbb{S}_S$ is the unit sphere in $\mathbb{R}^S$, while $\text{vol}_S(\cdot)$ means volume in $S$ dimensions. This definition is equivalent to the one in equation S22 [30].

These two equivalent definitions can be expressed in terms of an integral in the space of the growth rate vectors:

$$\Xi = \frac{2^S}{\text{vol}_{S-1}(\mathbb{S}_S)} \int_{\mathbb{R}^S} d^S\mathbf{r} \, 2\|\mathbf{r}\| \, \delta(\|\mathbf{r}\|^2 - 1) \prod_{i=1}^{S} \Theta(n_i^*(\mathbf{r})) \,, \tag{S24}$$

where $\text{vol}_{S-1}(\mathbb{S}_S)$ is the volume of the unit sphere's surface in $S$ dimensions, $\Theta(\cdot)$ is the Heaviside function (equal to 1 is the argument is positive and to zero otherwise), and $\delta(\cdot)$ is the Dirac delta function. In this expression, we integrate over the surface of the $S$-dimensional unit sphere. The integral of a function $f(\mathbf{x})$ on the unit sphere is given by

$$\int_{\mathbb{S}_S} d^S\mathbf{x} \, f(\mathbf{x}) = \int_{\mathbb{R}^S} d^S\mathbf{x} \, 2\|\mathbf{x}\|\delta(\|\mathbf{x}\|^2 - 1) \, f(\mathbf{x}) \,, \tag{S25}$$

where the term $\delta(\|\mathbf{x}\|^2 - 1)$ that appears in the integration constrains $\mathbf{x}$ on the surface of the unit sphere, and the factor $2\|\mathbf{x}\|$ is the derivative of the delta function's argument, which is needed because the Dirac delta is nonlinear in $\|\mathbf{r}\|$. The factor $\text{vol}_{S-1}(\mathbb{S}_S)$, the surface of sphere in $S$ dimensions, can be obtained by setting $f(x) = 1$:

$$\text{vol}_{S-1}(\mathbb{S}_S) = \int d^S\mathbf{x} \, 2\|\mathbf{x}\|\delta(\|\mathbf{x}\|^2 - 1) = \frac{2\pi^{S/2}}{\Gamma(S/2)} \,, \tag{S26}$$

where $\Gamma(\cdot)$ is the Gamma function. Finally, the term $\prod_{i=1}^{S} \Theta(\mathbf{n}_i^*(\mathbf{r}))$ in equation S24 expresses the constraint of all $n_i^*$ having to be positive: this product is equal to 1 if the equilibrium $\mathbf{n}^*(\mathbf{r})$ is feasible and zero otherwise. The equilibrium $\mathbf{n}^*(\mathbf{r})$ is a function of $\mathbf{r}$ via equation S4.

Equation S24 defines $\Xi$ as the volume of the domain of growth rates leading to feasible solutions. Using the results of section S2, we know that if the interaction matrix $\mathbf{A}$ is nonreactive then a feasible fixed point is globally stable. In this case $\Xi$ is the volume of the domain of intrinsic growth rates leading to feasible and (globally) stable solutions.

Unfortunately, direct numerical computation of $\Xi$ is inefficient when the number of species $S$ is large. To evaluate the integral in equation S24, e.g., via Monte Carlo integration, we should draw intrinsic growth rates at random and count how many of them, out of the total, lead to a feasible equilibrium. In order to have a reliable estimate of this proportion, we should sample the space in such a way that the number of feasible growth rates found is large. This goal requires an exponentially increasing sampling effort as $S$ increases. In this section we provide an alternative, much faster and reliable, way of estimating $\Xi$.

The equilibrium solution and the growth rates are linearly related via $r_i = -\sum_{i=1}^{S} A_{ij} n_j^*$ (equation S3). Our strategy is to use this to perform a change of variables in equation S24, and integrate over $\mathbf{n}^*$ instead of $\mathbf{r}$. Since $\mathbf{A}$ is nonreactive (and thus stable and not singular), it is invertible, and so it is always possible to perform this change of variables. We then obtain

$$\Xi = \frac{2^S \, \Gamma(S/2) \, |\det(\mathbf{A})|}{2\pi^{S/2}} \int_{\mathbb{R}^S} d^S\mathbf{n}^* \, 2\delta\left(\sum_{i,j,k} n_i^* A_{ki} A_{kj} n_j^* - 1\right) \prod_{i=1}^{S} \Theta(n_i^*) \,, \tag{S27}$$

where $|\det(\mathbf{A})|$ is the determinant of $\mathbf{A}$, which is also the Jacobian of the change of variables. After the change of variables, the integration is now performed over the feasible equilibrium points and so the condition of feasibility is automatically implemented.

It is still difficult to evaluate the previous expression numerically, because of the constraint that appears in the delta function. We can further simplify it by introducing polar coordinates. In particular, we write the vector $\mathbf{n}$ as $\mathbf{n} = n\mathbf{u}$, where $n = \|\mathbf{n}\|$ and $\mathbf{u}$ is a vector of unit length. We can perform a new change of variables, passing from $\mathbf{n}$ to $n$ and $\mathbf{u}$. Specifically, for any function $f(\mathbf{n})$, we can write

$$\int_{\mathbb{R}^S} \mathrm{d}^S\mathbf{n} \, f(\mathbf{n}) = \int_0^\infty \mathrm{d}n \, n^{S-1} \int_{\mathbb{R}^S} \mathrm{d}^S\mathbf{u} \, 2\delta(\|\mathbf{u}\|^2 - 1)f(n\mathbf{u}) = \int_0^\infty \mathrm{d}n \, n^{S-1} \int_{\mathbb{S}_S} \mathrm{d}^S\mathbf{u} \, f(n\mathbf{u}) \, . \tag{S28}$$

Using this expression in equation S27, we obtain

$$\Xi = \frac{2^S \, \Gamma(S/2) \, \det(\mathbf{A})}{2\pi^{S/2}} \int_0^\infty \mathrm{d}n \, n^{S-1} \int_{\mathbb{S}_S} \mathrm{d}^S\mathbf{u} \, 2\delta\left(n^2 \sum_{i,j} u_i G_{ij} u_j - 1\right) \prod_{i=1}^S \Theta(u_i) \, , \tag{S29}$$

where we used the fact that $\Theta(n_i) = \Theta(u_i)$ (since $n_i = nu_i$, and $n$ is positive by definition), and we have introduced the matrix $G_{ij} = \sum_k A_{ki}A_{kj}$. We can now perform the integration over $n$, obtaining

$$\int_0^\infty \mathrm{d}n \, n^{S-1} \, 2 \, \delta\left(n^2 \sum_{i,j} u_i G_{ij} u_j - 1\right) =$$
$$= \int_0^\infty \mathrm{d}n \, n^{S-1} \, 2 \, \delta\left(n - \frac{1}{\sqrt{\sum_{i,j} u_i G_{ij} u_j}}\right) \frac{1}{2n \sum_{i,j} u_i G_{ij} u_j} = \left(\sum_{i,j} u_i G_{ij} u_j\right)^{-S/2} \, , \tag{S30}$$

and therefore the integral of equation S24 finally reads

$$\Xi = \frac{2^S \, \Gamma(S/2) \, \sqrt{\det(\mathbf{G})}}{2\pi^{S/2}} \int_{\mathbb{S}_S} \mathrm{d}^S\mathbf{u} \, \prod_{i=1}^S \Theta(u_i) \left(\sum_{i,j} u_i G_{ij} u_j\right)^{-S/2} \, , \tag{S31}$$

where we have used the fact that $\det(\mathbf{G}) = \det(\mathbf{A}^t \mathbf{A}) = \det(\mathbf{A})^2$. In terms of the interaction matrix, the equation reads

$$\Xi = \frac{2^S \, \Gamma(S/2) \, |\det(\mathbf{A})|}{2\pi^{S/2}} \int_{\mathbb{S}_S} \mathrm{d}^S\mathbf{u} \, \prod_{i=1}^S \Theta(u_i) \left(\sum_{i,j,k} u_i A_{ki} A_{kj} u_j\right)^{-S/2} \, . \tag{S32}$$

Equation S31 shows explicitly the role of the generators. The matrix $\mathbf{G}$ can indeed be rewritten as

$$G_{ik} = \sum_j g_j^i g_j^k c_i c_k = c_i c_k \mathbf{g}^i \cdot \mathbf{g}^k \, , \tag{S33}$$

where $g_j^k$ are the generators of the convex cone defined in equation S12 and $c_i$ are arbitrary positive constants. Their presence, which can be seen as a change of the normalization of the vectors $\mathbf{g}^k$, does not affect the form of equation S31 and its dependence on $\mathbf{G}$ (see section S3). This property can be checked explicitly from equation S31, by introducing an explicit dependence on $c_i$ and showing that $\Xi$ is independent of their values.

Unfortunately, the integral in equation S31 cannot be computed analytically. As mentioned before, when the integral is written in the form of equation S24 it is impractical to evaluate it numerically, since it would require an exponentially increasing sampling to get a reasonable precision. Fortunately, this is not the case when the integral is written as in equations S31 and S32. The main difference is that, after changing variables, we are directly sampling the space of feasible solutions, without losing computational time in randomly exploring the space of intrinsic growth rates looking for feasible solutions.

To evaluate the integral, we use the usual approach of Monte Carlo algorithms. In particular, it is possible to write the integral as an average over random points:

$$\frac{1}{T}\sum_{a=1}^{T}\left(\sum_{i,j}u_i^a G_{ij}u_j^a\right)^{-S/2} \to \frac{\Gamma(S/2)}{2\pi^{S/2}}\int d^S u \prod_{i=1}^{S}\Theta(u_i)\, 2\delta(\|u\|^2-1)\left(\sum_{i,j}u_i G_{ij}u_j\right)^{-S/2} \tag{S34}$$

when $T \to \infty$. In this expression $\mathbf{u}^a$ are independently drawn random vectors uniformly distributed on the unit sphere and with only positive components. These two conditions are introduced to satisfy the constraints $\prod_{i=1}^{S}\Theta(u_i)$ and $2\delta(\|u\|^2-1)$ that appear in the integral. $T$ is the sample size, and the average on the left hand side of equation S34 converges to the right hand side in the large $T$ limit.

One always has a finite sample size $T$, used to approximate the integral. It is therefore important to have an estimate of the error made due to $T < \infty$. Since the left hand side of equation S34 is an average of a function over random vectors, this error can be estimated by simply using the variance of the function's values. In particular, the error $\sigma_{\text{MC}}$ is defined as

$$\sigma_{\text{MC}} = \frac{1}{\sqrt{T}}\sqrt{\frac{1}{T}\sum_{a=1}^{T}\left(\sum_{i,j}u_i^a G_{ij}u_j^a\right)^{-S} - \left(\frac{1}{T}\sum_{a=1}^{T}\left(\sum_{i,j}u_i^a G_{ij}u_j^a\right)^{-S/2}\right)^2}. \tag{S35}$$

The numerical simulation presented in the work where obtained were obtained with different sampling effort $T$. Instead of fixing $T$ a priori, we determined a precision goal, that we measured in terms of the relative error $\sigma_{MC}/\Xi$. We ran the simulations until $\sigma_{MC}/\Xi < 0.05$. In order to avoid artificially small samples and to have enough statistical power not to undershoot to much $\sigma_{\text{MC}}$, we ran $10 \times S$ Monte Carlo steps before checking the condition for the first time.

## S5. STABILITY, REACTIVITY, AND FEASIBILITY IN RANDOM MATRICES

Random matrices are a useful tool in ecology, and have been studied since May's seminal paper [8]. Mostly, they have been used to model the community matrix [8, 9]. In the context of this work, we use random matrices to model interaction matrices $\mathbf{A}$. We consider random matrices constructed in the following way:

- $A_{ii} = -d$ where $d$ is a positive constant.

- Each pair $(A_{ij}, A_{ji})$ is set equal to a pair of random variables drawn from a joint distribution with probability density function $q(x, y)$.

- The random variables are exchangeable—i.e., the probability distribution function is symmetric in its arguments: $q(x, y) = q(y, x)$—and all the moments are finite.

We show that the three most important quantities for our problem are the moments

$$E_1 = \int \mathrm{d}x \ \mathrm{d}y \ xq(x, y) = \int \mathrm{d}x \ \mathrm{d}y \ yq(x, y) \ , \tag{S36}$$

$$E_2 = \sqrt{\int \mathrm{d}x \ \mathrm{d}y \ (x - E_1)^2 q(x, y)} = \sqrt{\int \mathrm{d}x \ \mathrm{d}y \ (y - E_1)^2 q(x, y)} \ , \tag{S37}$$

$$E_c = \frac{1}{E_2^2} \int \mathrm{d}x \ \mathrm{d}y \ (x - E_1)(y - E_1)q(x, y) \ . \tag{S38}$$

In the limit of large $S$, they can be computed as proper sample means of $\mathbf{A}$'s entries:

$$E_1 = \frac{1}{S(S - 1)} \sum_{i=1}^{S} \sum_{j \neq i} A_{ij} \ , \tag{S39}$$

$$E_2 = \sqrt{\frac{1}{S(S - 1)} \sum_{i=1}^{S} \sum_{j \neq i} (A_{ij})^2 - E_1^2} \ , \tag{S40}$$

$$E_c = \frac{1}{E_2^2} \left( \frac{1}{S(S - 1)} \sum_{i=1}^{S} \sum_{j \neq i} A_{ij} A_{ji} - E_1^2 \right) \ . \tag{S41}$$

The parameterization used by May [8] would correspond to

$$q_{\mathrm{May}}(x, y) = \Big( (1 - C)\delta(x) + Cp(x) \Big) \Big( (1 - C)\delta(y) + Cp(y) \Big) \ , \tag{S42}$$

where $\delta(\cdot)$ is the Dirac delta function and $p(x)$ is an arbitrary distribution with mean zero and variance $\sigma^2$. The connectance $C$ sets the probability that each entry is equal to zero (with probability $1 - C$) or randomly drawn from the probability distribution $p(x)$ with probability $C$. In this case $E_1 = E_c = 0$, while $E_2^2 = C\sigma^2$.

In the following, we summarize known results on the spectra, reactivity conditions, and properties of $\Xi$ for these matrices.

### A.  Known results on the spectra of random matrices

Under the assumptions of the previous section, the eigenvalues of $\mathbf{A}$ in the limit of large $S$ are uniformly distributed in an ellipse in the complex plane. If $E_1 \neq 0$ there is always an eigenvalue $\lambda_m$ whose value is approximately

$$\lambda_m \approx -d + SE_1 \ , \tag{S43}$$

independently of the rest of the eigenvalue distribution. The ellipse is centered at $-d - E_1$, its axes are aligned with the real and imaginary axes, and their lengths are

$$a = \sqrt{S} E_2 (1 + E_c) \tag{S44}$$

and

$$b = \sqrt{S} E_2 (1 - E_c) . \tag{S45}$$

If $\lambda_m = 0$, the eigenvalue with the largest real part(s) is approximated by the rightmost point of the ellipse. The system is stable if its real part is negative. In the most general case, this condition is equivalent to

$$-d + \max \left\{ SE_1, -E_1 + \sqrt{S} E_2 (1 + E_c) \right\} < 0 . \tag{S46}$$

In section S2 we introduced the concept of reactivity. In particular, we showed that when the matrix is not reactive then it is possible to disentangle stability and feasibility. The matrix is nonreactive if the eigenvalues of $\mathbf{A} + \mathbf{A}^t$ are all negative. This condition reads [15]

$$-d + \max \left\{ SE_1, -E_1 + \sqrt{2S(1 + E_c)} E_2 \right\} < 0 . \tag{S47}$$

Figure S1 shows the values of parameters leading to the possible combinations of stability and reactivity in random matrices for the case $E_1 = 0$. Since we imposed the condition of nonreactivity of the matrix $\mathbf{A}$, the region of parameters we explore is the one above the reactivity line. One can see that in this way we are missing some parameterizations, corresponding to those that lead to a stable reactive system. From equations S46 and S47 one can see that the case $E_1 < 0$ is very similar to the case $E_1 = 0$. More interestingly, for $E_1 > 0$, the conditions for stability and reactivity converge in the large $S$ limit, implying that we are considering all the possible cases.

What is remarkable in these conditions and in the distribution of eigenvalues is that they are *universal* [17, 31–33]. Universality means that they depend only on $S$, $E_1$, $E_2$, and $E_c$ (and $d$, but via a trivial dependence). The spectrum of eigenvalues does not depend on the detailed form of the distribution $q(x, y)$.

For instance, consider the case $q(x, y) = p(x)p(y)$, where the upper and lower triangular entries $A_{ij}$ and $A_{ji}$ are independent random variables. In this case $E_c = 0$ and $E_1$ and $E_2$ are the mean and standard deviation of the distribution $p(x)$. The distribution of eigenvalues and the conditions for stability and reactivity are the same for *any* probability distribution $p(x)$ as long as their mean $E_1$ and standard deviation $E_2$ are the same (provided some mild conditions on higher moments hold). For instance, a Lognormal distribution, a Gaussian distribution and an exponential distribution, having same mean and standard deviation, produce the same eigenvalue distribution, and therefore the same conditions for stability [34].

From an ecological perspective, one can consider different interaction matrices corresponding to different interaction types. The interaction type is given by the signs of the pairs $(A_{ij}, A_{ji})$: competitive interactions will have both entries
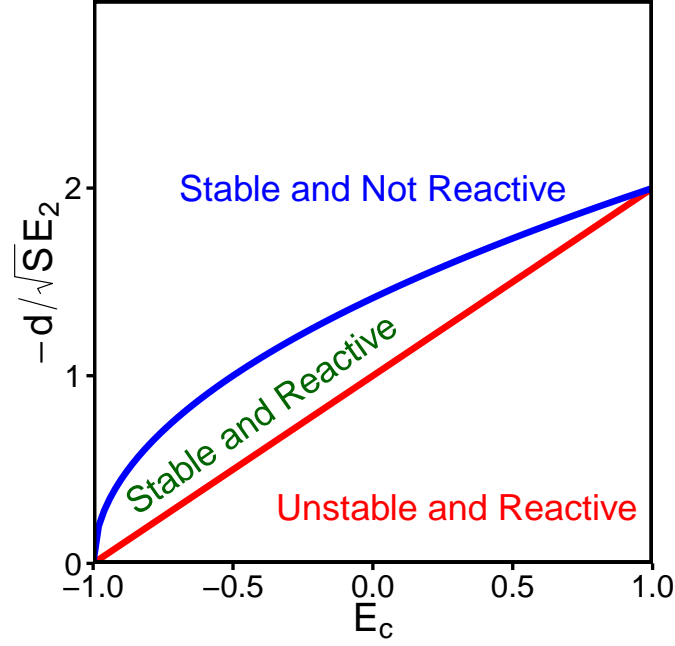
Supplementary Figure S1: Reactivity and stability for random matrices in the case $E_1 = 0$. The red curve describes the condition for stability (equation S46), while the blue curve corresponds to the reactivity condition (equation S47). The region above the blue curve corresponds to parameterizations that are both stable and nonreactive, while the region below the red curve corresponds to unstable and reactive matrices. The parameterizations that may still lead to stabille and feasible points but we are not considering are in the region between the two curves. The shape of this region does not change substantially if $S$ and $E_2$ are changed or if $E_1 < 0$. For $E_1 > 0$ the reactive stable region is always smaller and eventually disappears (i.e., the blue and the red curve become the same) when $S$ is large enough.

with a negative sign, while in trophic interactions the entries will have opposite sign. The interaction pairs $(A_{ij}, A_{ji})$ for competitive interactions can for instance be obtained from the following distribution:

$$q_{\text{comp}}(x, y) = (1 - C)\delta(x)\delta(y) + C h_-(x)h_-(y) , \tag{S48}$$

where $h_-$ is a probability distribution function with support on the negative axis (i.e., the random variables are always negative), and $C$ is the connectance (a pair is different from zero with probability $C$). In the case of trophic interactions we could consider

$$q_{\text{troph}}(x, y) = (1 - C)\delta(x)\delta(y) + \frac{C}{2}p_-(x)p_+(y) + \frac{C}{2}p_+(x)p_-(y) , \tag{S49}$$

where $p_+$ and $p_-$ are two probability distribution functions with positive and negative support, respectively. Suppose that the moments of $h_-$, $p_+$, and $p_-$ are chosen in such a way that $q_{\text{comp}}(x, y)$ and $q_{\text{troph}}(x, y)$ have the same values of $E_1$, $E_2$, and $E_c$. The interaction matrices will still look very different in the two cases: one describes a foodweb and the other a competitive system. Despite this difference, the two will have the same stability properties. In other

words, different interaction types influence the stability properties of the system only via $E_1$, $E_2$ and $E_c$.

## B.   Universality of $\Xi$

In this section we show that, apart from their spectral distribution, $\Xi$ is also a universal quantity in large random matrices. That is, in the large $S$ limit, its value does not depend on the entire distribution of the coefficients, but only on the three moments $E_1$, $E_2$, and $E_c$. It is important to remark that this result applies to the large $S$ limit: the sub-leading corrections depend in principle on all the moments.

In order to show that $\Xi$ is universal, we parameterized random networks with different distributions and checked whether $\Xi$ depends only on $E_1$, $E_2$, $E_c$, and $S$, but not on other properties. To do this, we constructed several $S \times S$ matrices. Each individual matrix had its entries drawn from some fixed distribution, but the shape of the distribution was different across matrices. However, regardless of the distribution's shape, their moments were fixed at $E_1$, $E_2$, and $E_c$. We then checked whether these matrices led to the same value of $\Xi$.

In our simulations we considered a distribution of the pairs $(A_{ij}, A_{ji})$ of the form

$$q(x, y) = (1 - C)\delta(x)\delta(y) + Cp(x, y) , \tag{S50}$$

where the connectance $C$ is the probability that two species $i$ and $j$ interact. The probability distribution $p(x, y)$ in equation S50 depends on three parameters $\mu$, $\sigma$, and $\rho$, which define the mean, variance, and correlation of the pairs drawn from $p(x, y)$. Given the values of $E_1$, $E_2$, and $E_c$, we can arbitrary choose $C$ and tune $\mu$, $\sigma$, and $\rho$ to obtain any desired $E_1$, $E_2$, and $E_c$. If $\Xi$ is universal, then different matrices built with different values of $C$, $\mu$, $\sigma$, and $\rho$ but the same values of $E_1$, $E_2$, and $E_c$ will lead to the same $\Xi$.

We considered five parameterizations of the distribution $p(x, y)$:

- Random signs, normal distribution:

$$p(x, y) = BN(x, y|\mu, \sigma, \rho) . \tag{S51}$$

  The distribution $BN(x, y|\mu, \sigma, \rho)$ is a bivariate normal distribution with marginal means equal to $\mu$, marginal variances equal to $\sigma^2$, and correlation equal to $\rho\sigma^2$. The pairs can in principle assume all possible combinations of signs.

- Random signs, four corners:

$$\begin{aligned}p(x, y) =& \frac{q}{2}\delta(x - \mu - \sigma)\delta(y - \mu - \sigma) + \frac{q}{2}\delta(x - \mu + \sigma)\delta(y - \mu + \sigma) \\ &+ \frac{1 - q}{2}\delta(x - \mu - \sigma)\delta(y - \mu + \sigma) + \frac{1 - q}{2}\delta(x - \mu + \sigma)\delta(y - \mu - \sigma) .\end{aligned} \tag{S52}$$

  The pairs $(x, y)$ can take on only four different, discrete values, potentially corresponding to all combinations on signs. The probability distribution depends on three parameters $\mu$ and $\sigma^2$ are means an variances of the distribution, while the correlation $\rho\sigma^2$ can be obtained from $\rho = 2q - 1$.

- $(+,+)$, Lognormal:

$$p(x,y) = LBN(x,y|\mu,\sigma,\rho) \ . \tag{S53}$$

The distribution $LBN(x,y|\mu,\sigma,\rho)$ is a bivariate lognormal distribution with marginal means equal to $\mu > 0$, marginal variances equal to $\sigma^2$, and correlation equal to $\rho\sigma^2$. The pairs can in principle assume only positive signs. Note that not all values of $\rho$ between $-1$ and $1$ can be obtained when a Lognormal distribution is considered.

- $(-,-)$, Lognormal:

$$p(x,y) = LBN(-x,-y|-\mu,\sigma,\rho) \ . \tag{S54}$$

This distribution takes the values drawn from a bivariate lognormal distribution, times $-1$. It has marginal means equal to $\mu < 0$, marginal variances equal to $\sigma^2$, and correlation equal to $\rho\sigma^2$. The pairs assume only negative signs. Note that not all values of $\rho$ between $-1$ and $1$ can be obtained when a Lognormal distribution is considered.

- $(+,-)$, Lognormal:

$$\begin{aligned} p(x,y) = &\frac{1}{2}LN(x|\mu_1,(1+\rho)\sigma)LN(-y|-\mu_2,(1+\rho)\sigma) \\ &+\frac{1}{2}LN(y|\mu_1,(1+\rho)\sigma)LN(-x|-\mu_2,(1+\rho)\sigma) \ . \end{aligned} \tag{S55}$$

The distribution $LN(x|\mu,\sigma)$ is Lognormal distribution with mean $\mu_1 + \mu_2$ (where $\mu_1 > 0$ and $\mu_2 < 0$), variance $\sigma^2$, and correlation $\rho\sigma^2$. The pairs assume only values with opposite signs $(+,-)$ or $(-,+)$.

In ecological terms, the first two distributions correspond to a random community (where the signs of the interaction strength are random), the $(+,+)$ case corresponds to a mutualistic community, $(-,-)$ to a competitive community, while $(+,-)$ corresponds to a food web. The mutualistic/competitive matrices can lead only to positive/negative means $E_1$, respectively, while the other settings can produce arbitrarily values of $E_1$.

Figure S2 shows the value of $\Xi$ and of the largest eigenvalue $\lambda$ for interaction matrices constructed with different connectances $C$ and distributions, but with the same values of $E_1$, $E_2$, and $E_c$. As seen from the figure, the values of $\Xi$ and $\lambda$ in any particular case match up precisely with the average values over several different realizations, demonstrating that these two quantities are indeed universal.
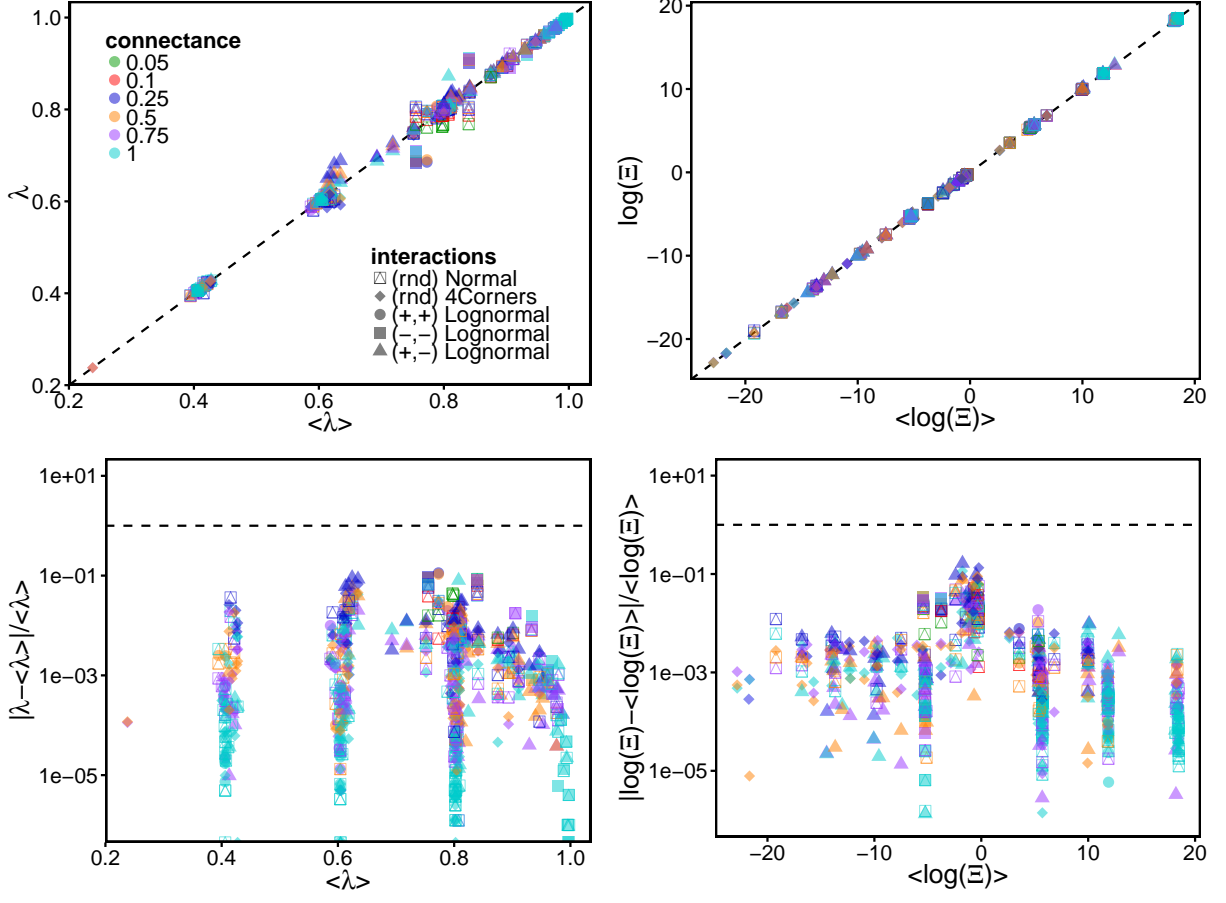
Supplementary Figure S2: Universality of $\lambda$ and $\Xi$ in random matrices. The two left panels refer to the eigenvalue with the largest real part $\lambda$ of the interaction matrix $\mathbf{A}$, while the right ones to the size of the feasibility domain $\Xi$. We consider different values of the connectance (colors) and different distributions (shape), such that there were multiple combination of connectances and distributions having the same values of $E_1$, $E_2$, and $E_c$. We computed the averages $\langle \lambda \rangle$ and $\langle \log(\Xi) \rangle$ over all realizations of the matrices having the same values of $E_1$, $E_2$, and $E_c$. If the value of $\lambda$ and $\Xi$ are universal, then they depend only on $E_1$, $E_2$, and $E_c$, and therefore their values are equal to the mean: universality holds if $\lambda = \langle \lambda \rangle$ and $\log(\Xi) = \langle \log(\Xi) \rangle$. The top panels show that these two quantities are equal and the bottom panels quantify their deviations. We know that $\lambda$ is universal, and since $\Xi$ has a similar behavior, we conclude that $\Xi$ is also universal.

## S6. MEAN-FIELD APPROXIMATION OF $\Xi$

The goal of this section is to compute an approximation for $\Xi$ in the limit of large $S$. The volume $\Xi$ is defined (see section S4) as

$$\Xi = \frac{2^S \; \Gamma(S/2) \; \sqrt{\det(\mathbf{G})}}{2\pi^{S/2}} \int_{\mathbb{S}_S} \mathrm{d}^S \mathbf{u} \; \prod_{i=1}^{S} \Theta(u_i) \left( \sum_{i,j} u_i G_{ij} u_j \right)^{-S/2} , \tag{S56}$$

where the matrix $\mathbf{G}$ can be obtained from the generators of the polytope (see equations S12 and S33), and therefore from the interaction matrix $\mathbf{A}$.

We can introduce a Gaussian function in equation S56 using the fact that, for any positive constant $c$,

$$c^{-S/2} = \frac{2}{\Gamma(S/2)} \int_0^\infty \mathrm{d}r \; r^{S-1} \exp(-cr^2) \; . \tag{S57}$$

Introducing this Gaussian integral in equation S56 by letting $c = \sum_{i,j} u_i G_{ij} u_j$, we obtain

$$\Xi = \sqrt{\det(\mathbf{G})} \left(\frac{2}{\sqrt{\pi}}\right)^S \int_0^\infty \mathrm{d}r \; r^{S-1} \int_{\mathbb{S}_S} \mathrm{d}^S \mathbf{u} \; \left(\prod_{i=1}^S \Theta(u_i)\right) \; \exp\left(-r^2 \sum_{i,j} u_i G_{ij} u_j\right) \; , \tag{S58}$$

which can be rewritten as

$$\Xi = \sqrt{\det(\mathbf{G})} \left(\frac{2}{\sqrt{\pi}}\right)^S \int_{\mathbb{R}^S} \mathrm{d}^S \mathbf{z} \; \left(\prod_{i=1}^S \Theta(z_i)\right) \; \exp\left(-\sum_{i,j} z_i G_{ij} z_j\right) \; , \tag{S59}$$

where $z_i = r u_i$. We can rewrite this equation as

$$\Xi = \sqrt{\det(\mathbf{G})} \left(\frac{2}{\sqrt{\pi}}\right)^S \int_{\mathbb{R}^S} \mathrm{d}^S \mathbf{z} \; \prod_{i=1}^S \left(\Theta(z_i) \; e^{-z_i^2} \exp\left(-\sum_{j \neq i} z_i G_{ij} z_j\right)\right) \; , \tag{S60}$$

where we used the fact that the diagonal entries of $\mathbf{G}$, when expressed in terms of the normalized generators, are equal to one.

The reader familiar with statistical mechanics will notice that equation S60, which can be written as

$$\Xi \propto \int_{\mathbb{R}^S} \mathrm{d}^S \mathbf{z} \; q(\mathbf{z}) \prod_{i=1}^S \left(\exp\left(-\sum_{j \neq i} z_i G_{ij} z_j\right)\right) \; , \tag{S61}$$

has the form of a partition function. For instance one can recover the Ising model [35] with the choice $q(\mathbf{z}) = \prod_i \delta(z_i^2 = 1)$ or the spherical model [36] when $q(\mathbf{z}) = \delta(S - \sum_i z_i^2)$. The term $z_i G_{ij} z_j$ in particular plays the role of the interactions of the system.

Integrals of the form S61 are the most studied objects of statistical mechanics, and yet in most cases are not analytically solvable. There are, on the other hand, many techniques that can be used to obtain good approximations to S61. The most celebrated one is probably the mean-field approximation [35] and it is the one we are using in this section. In particular, the idea of the mean-field approximation is to replace the interactions of an entity (spins in the case of the Ising model or species in our case) with an average "effective" interaction. This reduces a many-body problem, where all interactions of spins or populations are coupled, into an effective one-body problem.

If the system is large enough (in our case if $S \to \infty$), the mean-field approximation is know to be exact in the case of "fully connected" interactions. In terms of equation S61, this corresponds to a matrix $\mathbf{G}$ with the same constant in all its offdiagonal entries. The matrix $\mathbf{G}$ is constant when $\mathbf{A}$ has constant offdiagonal entries. We will consider therefore the case of $\mathbf{A}$'s diagonal entries being equal to $-1$ and its offdiagonal entries to a constant $E_1$. Using equation S12, the $i$th component of the $k$th generator is then

$$g_i^k = -\frac{E_1}{1 + (S-1)E_1^2} \tag{S62}$$

for $i \neq k$, and

$$g_k^k = \frac{1}{1 + (S-1)E_1^2} \; . \tag{S63}$$

Using equation S33, we therefore obtain that the diagonal entries of $\mathbf{G}$ are equal to 1, while the offdiagonal ones are constant and equal to

$$G_{ij} = \frac{-2E_1 + (S-2)E_1^2}{1 + (S-1)E_1^2} \; . \tag{S64}$$

We define the constant $\beta$ as

$$\beta = S\frac{-2E_1 + (S-2)E_1^2}{1 + (S-1)E_1^2} \; , \tag{S65}$$

and therefore we have $G_{ii} = 1$ and $G_{ij} = \beta/S$ for $i \neq j$. The determinant of $\mathbf{G}$ in this case turns out to be

$$\det(\mathbf{G}) = \left(1 + \frac{S-1}{S}\beta\right)\left(1 - \frac{\beta}{S}\right)^{S-1} \approx (1+\beta)e^{-\beta} \; , \tag{S66}$$

where the last form holds for large $S$. In this case of constant interactions, we obtain, from equation S60,

$$\begin{aligned}
\Xi &= \sqrt{\det(\mathbf{G})}\left(\frac{2}{\sqrt{\pi}}\right)^S \int_{\mathbb{R}^S} \mathrm{d}^S\mathbf{z} \prod_{i=1}^S \left(\Theta(z_i)\, e^{-z_i^2} \exp\left(-z_i\frac{\beta}{S}\sum_{j\neq i} z_j\right)\right) = \\
&= \sqrt{\det(\mathbf{G})}\left(\frac{2}{\sqrt{\pi}}\right)^S \int_{\mathbb{R}^S} \mathrm{d}^S\mathbf{z} \left(\prod_{i=1}^S \Theta(z_i)\right) \exp\left(-\sum_i z_i^2 - \frac{\beta}{S}\left(\sum_i z_i\right)^2\right) \; ,
\end{aligned} \tag{S67}$$

up to subleading terms in $S$.

Equation S67 can be written as

$$\Xi = \sqrt{\det(\mathbf{G})}\left(\frac{2}{\sqrt{\pi}}\right)^S Z_h \left\langle \exp\left(-\frac{\beta}{S}\left(\sum_i z_i\right)^2 + h\sum_i z_i\right)\right\rangle_h \; , \tag{S68}$$

where

$$\begin{aligned}
Z_h &:= \int_{\mathbb{R}^S} \mathrm{d}^S\mathbf{z} \left(\prod_{i=1}^S \Theta(z_i)\right) \exp\left(-\sum_i z_i^2 - h\sum_i z_i\right) = \\
&= \left(\int_0^\infty \mathrm{d}z\, e^{-z^2-hz}\right)^S = \left(\frac{\sqrt{\pi}}{2}e^{h^2/4}\operatorname{erfc}(h/2)\right)^S \; ,
\end{aligned} \tag{S69}$$

where $\operatorname{erfc}(\cdot)$ is the complementary error function, defined as

$$\operatorname{erfc}(x) = \frac{2}{\sqrt{\pi}}\int_x^\infty \mathrm{d}t\, e^{-t^2} \; . \tag{S70}$$

The average $\langle\cdot\rangle_h$ is defined as

$$\left\langle f(\mathbf{z})\right\rangle_h := \frac{1}{Z_h}\int_{\mathbb{R}^S} \mathrm{d}^S\mathbf{z} \left(\prod_{i=1}^S \Theta(z_i)\right) \exp\left(-\sum_i z_i^2 - h\sum_i z_i\right) f(\mathbf{z}) \; . \tag{S71}$$

Using Jensen's inequality in equation S71 we have that

$$\Xi = \sqrt{\det(\mathbf{G})} \left(\frac{2}{\sqrt{\pi}}\right)^S Z_h \left\langle \exp\left(-\frac{\beta}{S}(\sum_i z_i)^2 + h\sum_i z_i\right)\right\rangle_h \geq$$
$$\geq \sqrt{\det(\mathbf{G})} \left(\frac{2}{\sqrt{\pi}}\right)^S Z_h \exp\left(\left\langle -\frac{\beta}{S}(\sum_i z_i)^2 + h\sum_i z_i\right\rangle_h\right) . \tag{S72}$$

In the following we will approximate the first expression with the second one. It is possible to prove that, in the large $S$ limit, the second expression converges to the first one.

Applying the mean-field approximation we neglect fluctuations of the variables, i.e. we have

$$\left\langle -\frac{\beta}{S}(\sum_i z_i)^2 + h\sum_i z_i\right\rangle_h = -\frac{\beta}{S}\left\langle(\sum_i z_i)^2\right\rangle_h + h\sum_i \langle z_i\rangle_h \approx S\left(-\beta m^2 + hm\right) , \tag{S73}$$

where

$$m := \langle z_i\rangle_h = -\frac{1}{S}\frac{\partial}{\partial h}\log(Z_h) . \tag{S74}$$

By introducing equation S73 in equation S72 we have

$$\Xi \approx \sqrt{\det(\mathbf{G})} Z_h \left(\frac{2}{\sqrt{\pi}}\exp\left(-\beta m^2 + hm\right)\right)^S = \Xi_{MF} . \tag{S75}$$

This equation is a function of $h$, which is a free parameter. Since it is a lower bound for the actual value of $\Xi$, the best approximation would correspond to the value of $h$ which maximizes the approximation. We have therefore that $h$ is a solution of the following equation

$$0 = \frac{\partial}{\partial h}\log(\Xi_{MF}) = \frac{\partial}{\partial h}\log(Z_h) + S\frac{\partial}{\partial h}(-\beta m^2 + hm) = S(h - 2\beta m)\frac{\partial m}{\partial h} , \tag{S76}$$

where $m$ is given by equation S74. We obtain therefore $m = h/(2\beta)$ and then, by neglecting sub-leading terms in $S$ and introducing $m = h/(2\beta)$ in equation S75

$$\frac{1}{S}\log\Xi_{MF} \approx \log\left(\mathrm{erfc}(h/2)\exp\left(\frac{h^2}{4}\frac{1+\beta}{\beta}\right)\right) . \tag{S77}$$

By maximizing this equation respect to $h$ we obtain

$$0 = \frac{\partial}{\partial h}\log(\Xi_{MF}) = \frac{h}{2}\left(\frac{1}{\beta}+1\right) + \frac{\partial}{\partial h}\log(\mathrm{erfc}(h/2)) = \frac{h}{2}\left(\frac{1}{\beta}+1\right) - \frac{e^{-h^2/4}}{\sqrt{\pi}\,\mathrm{erfc}(h/2)} . \tag{S78}$$

Equation S78 cannot be solved exactly. By expanding around $h = 0$ we obtain

$$0 = \frac{h}{2}\left(\frac{1}{\beta}+1\right) - \frac{1}{\sqrt{\pi}} - \frac{h}{\pi} , \tag{S79}$$

which is solved by

$$h = \frac{2\beta\sqrt{\pi}}{\pi + \beta(\pi - 2)} . \tag{S80}$$

One can observe that the solution $h = 0$ corresponds to $\beta = 0$, i.e. to a non-interacting ecosystem. Expanding around $h = 0$ is therefore meaningful when the interactions are not too strong. It is possible to verify that the approximate solution S80 is very close to the actual solution obtained by solving numerically equation S78 also for not too small values of $\beta$

Using equation S80 into equation S77 we obtain

$$\frac{1}{S} \log \Xi_{MF} \approx \frac{\beta(1+\beta)\pi}{(\pi + \beta(\pi - 2))^2} + \log \text{erfc}\left(\frac{\sqrt{\pi}\beta}{\pi + \beta(\pi - 2)}\right) \ , \tag{S81}$$

which is our final result. In figure S3 we compare this equation with the volume computed numerically in the case of constant interactions, finding a very good match.

In the most general case of an interaction matrix with nonconstant offdiagonal entries, we can consider equation S73 as an approximation valid in the case of $E_2 \to 0$. As $\beta$ was defined in terms of the generators, we can extend the approximation to the case $E_2 > 0$ by considering $\beta$ as the expected value of $\mathbf{G}$'s entries, which corresponds to the average overlap of two rows of the interaction matrix $\langle \cos(\eta) \rangle$, defined in equation S111. In this more general case the mean-field value of $\Xi$ is expected to be a good approximation when $\text{var}(\cos(\eta))$ is small enough. By substituting $\beta = \langle \cos(\eta) \rangle$, using equation S111, into equation S73 we obtain

$$\frac{1}{S} \log(\Xi) \approx \frac{\pi E_1 (2d - E_1 S)\left(2dE_1 + d - S\left(2E_1^2 + E_2^2\right)\right)}{\left(d(2(\pi - 2)E_1 + \pi) - S\left(2(\pi - 1)E_1^2 + \pi E_2^2\right)\right)^2}$$
$$\log\left(\text{erfc}\left(\frac{\sqrt{\pi}E_1(E_1 S - 2d)}{S\left(2(\pi - 1)E_1^2 + \pi E_2^2\right) - d(2(\pi - 2)E_1 + \pi)}\right)\right) \ . \tag{S82}$$

When $\text{var}(\cos(\eta))$ is not small, we observed that the empirical formula

$$\frac{1}{S} \log(\Xi) \approx \frac{\pi E_1 (2d - E_1 S)\left(2dE_1 + d - S\left(2E_1^2 + E_2^2\right)\right)}{\left(d(2(\pi - 2)E_1 + \pi) - S\left(2(\pi - 1)E_1^2 + \pi E_2^2\right)\right)^2}$$
$$\log\left(\text{erfc}\left(\frac{\sqrt{\pi}E_1(E_1 S - 2d)}{S\left(2(\pi - 1)E_1^2 + \pi E_2^2\right) - d(2(\pi - 2)E_1 + \pi)}\right)\right) +$$
$$+ \log\left(1 + \frac{3SE_2^2(1 + E_c)}{2\pi}\right) \ . \tag{S83}$$

explains well the values obtained in simulations. This is the formula we used to make figure 2 in the main text.

In order to simplify the expression and make it more readable, we can expand equation S84 around $\beta = 0$, i.e., when the interactions between species are small. By expanding $(\Xi_{MF})^{1/S}$ around $\beta = 0$ and taking the logarithm of the expression, we obtain

$$\frac{1}{S} \log \Xi_{MF} \approx \log\left(1 - \frac{\beta}{\pi}\right) \ . \tag{S84}$$

Equation 2 of the main text was obtained by substituting $\beta = \langle \cos(\eta) \rangle$, using equation S111, in the case of $E_2 = 0$.

## S7. EMPIRICAL NETWORKS AND RANDOMIZATIONS

We considered 89 mutualistic networks and 15 food webs. Empirical networks are encoded in terms of adjacency matrices $\mathbf{L}$, with $L_{ij} = 1$ if species $j$ affects species $i$ and zero otherwise.
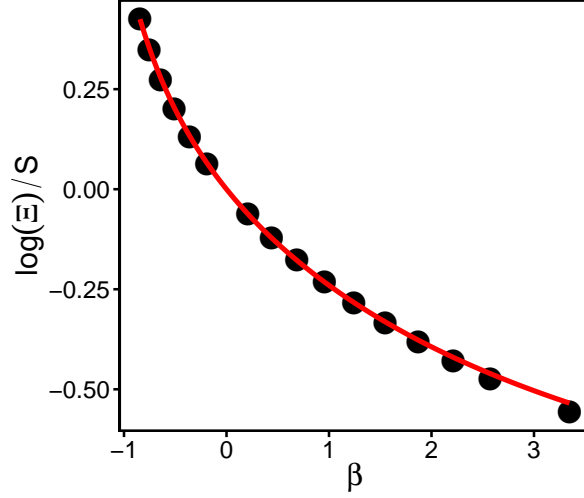
Supplementary Figure S3: Approximation of $\Xi$ using mean field theory. The black dots are numerical simulations obtained by integrating $\Xi$ numerically (see section S4) for a constant interaction matrix. The red curve is the analytical approximation obtained using the mean-field approximation (see equation S82). $\beta$ is a function of $E_1$ and $S$, and is defined in equation S65. The range of $\beta$ considered here is the same of the one appearing in figure 1 of the main text.

## A.  Mutualistic networks

The 89 mutualistic networks (59 pollination networks and 30 seed-dispersal networks) were obtained from the Web of Life dataset (`www.web-of-life.es`), where references to the original works can be found. When the original network was not fully connected, we considered the largest connected component.

In the case of mutualistic networks, the adjacency matrix $\mathbf{L}$ is bipartite, i.e., it has the structure

$$
\mathbf{L} = \begin{pmatrix} 0 & \mathbf{L}_b \\ \mathbf{L}_b^t & 0 \end{pmatrix} , \tag{S85}
$$

where $\mathbf{L}_b$ is a $S_A \times S_P$ matrix ($S_A$ and $S_P$ being the number of animals and plants respectively). The adjacency matrix contains information only about the interactions between animals and plants, but not about competition within plants or animals.

We parameterized the interaction matrix in the following way:

$$
\mathbf{A} = \begin{pmatrix} \mathbf{W}^A & \mathbf{L}_b \circ \mathbf{W}^{AP} \\ \mathbf{L}_b^t \circ \mathbf{W}^{PA} & \mathbf{W}^P \end{pmatrix} , \tag{S86}
$$

where the symbol $\circ$ indicates the Hadamard or entrywise product (i.e., $(\mathbf{A} \circ \mathbf{B})_{ij} = A_{ij} B_{ij}$), while $\mathbf{W}^A$, $\mathbf{W}^{AP}$, $\mathbf{W}^{PA}$, and $\mathbf{W}^P$ are all random matrices. $\mathbf{W}^A$ and $\mathbf{W}^P$ are both square matrices (of dimension $S_A \times S_A$ and $S_P \times S_P$), while $\mathbf{W}^{AP}$ and $\mathbf{W}^{PA}$ are rectangular matrices of size $S_A \times S_P$ and $S_P \times S_A$ respectively. The diagonal elements $W_{ii}^A$

and $W_{ii}^P$ were set to $-1$, while the pairs $(W_{ij}^A, W_{ji}^A)$ and $(W_{ij}^P, W_{ji}^P)$ were drawn from a bivariate normal distribution with mean $\mu_-$, variance $\sigma_+^2 = c\mu_-^2$, and correlation $\rho\sigma_+^2$. Since these two matrices represent competitive interactions, $\mu_- < 0$. The the pairs $(W_{ij}^{AP}, W_{ji}^{PA})$ were extracted from a bivariate normal distribution with mean $\mu_+$, variance $\sigma_-^2 = c\mu_+^2$, and correlation $\rho\sigma_-^2$, where $\mu_+ > 0$.

We analyze more than 600 parameterizations, obtained by considering different values of $\mu_-$, $\mu_+$, $c$, and $\rho$. We compared the results obtained for empirical networks with the corresponding randomizations. For each network we randomized the block $\mathbf{L}_b$ 1000 times, by generating connected networks with same size and number of links. We parameterized each randomized network independently as described above, and we compared their properties with those of the empirical network, parameterized independently 1000 times.

## B. Food webs

A summary of the properties and reference of the food webs can be found in table S1. In the case of food webs the adjacency matrix $L$ is not symmetric, and an entry $L_{ij} = 1$ indicates that species $j$ consumes species $i$. We removed all cannibalistic loops. Since both $L_{ij}$ and $L_{ji}$ are never simultaneously equal to one (there are no loops of length two), we parameterized the offdiagonal entries of $\mathbf{A}$ as

$$A_{ij} = W_{ij}^+ L_{ij} + W_{ji}^- L_{ji} \ , \tag{S87}$$

while the diagonal was fixed at $-1$. Both $\mathbf{W}^+$ and $\mathbf{W}^-$ are random matrices, where the pairs $(W_{ij}^+, W_{ij}^-)$ are drawn from a bivariate normal distribution with marginal means $(\mu_+, \mu_-)$ and correlation matrix

$$\begin{pmatrix} c\mu_+^2 & \rho c\mu_+^2 \\ \rho c\mu_-^2 & c\mu_-^2 \end{pmatrix} \tag{S88}$$

We analyzed more than 200 parameterizations, obtained by considering different values of $\mu_-$, $\mu_+$, $c$, and $\rho$. We then compared the results obtained for empirical networks with the corresponding randomizations. For each network, we randomized the adjacency matrix $\mathbf{L}$ 1000 times, by generating connected networks with the same size and number of links (and $\mathbf{L}\,\mathbf{L}^t = 0$). We parameterized each randomized network independently in way described above, and we compared their properties with those of the empirical network, parameterized independently 1000 times.

## S8.   POSSIBLE BIASES IN PREVIOUS ANALYSIS OF STRUCTURAL STABILITY

In section S4 we showed how to estimate the feasibility domain numerically in a fast and reliable way. In previous approaches [14], the feasibility domain (structural stability) was not directly calculated, but approximately inferred using a regression method. Using our new approach, we obtain different results from the ones obtained earlier [14]. In this section we show that the method used by Rohr et al. [14] could be biased and is not always applicable.

Supplementary Table S1: References and facts about the 15 food webs analyzed in the work

| Name | S | Number of links | Connectance |
|---|---|---|---|
| Ythan Estuary [37] | 92 | 414 | 0.1 |
| St. Marks [38] | 143 | 1763 | 0.17 |
| Grande Cariçaie [39] | 163 | 2048 | 0.16 |
| Serengeti [40] | 170 | 585 | 0.04 |
| Flensburg Fjord [41] | 180 | 1567 | 0.1 |
| Otago Harbour [42] | 180 | 1856 | 0.12 |
| Little Rock Lake [43] | 181 | 2316 | 0.14 |
| Sylt tidal basin [44] | 230 | 3298 | 0.12 |
| Caribbean Reef [45] | 249 | 3293 | 0.11 |
| Kongs Fjorden [46] | 270 | 1632 | 0.04 |
| Carpinteria Salt Marsh [47] | 273 | 3878 | 0.1 |
| San Quintin [47] | 290 | 3934 | 0.09 |
| Lough Hyne [48] | 349 | 5088 | 0.08 |
| Punta Banda [47] | 356 | 5291 | 0.09 |
| Weddell Sea [49] | 488 | 15435 | 0.13 |

The Authors considered a bipartite mutualistic system described by the dynamical model

$$
\begin{cases}
\dfrac{dn_i^A}{dt} = n_i^A \left( r_i^A - \sum_{j=1}^{S_A} \beta_{ij}^A n_j^A + \dfrac{\sum_{j=1}^{S_P} \gamma_{ij}^A n_j^P}{1 + h_i^A \sum_{j=1}^{S_P} \gamma_{ij}^A n_j^P} \right) \\
\dfrac{dn_i^A}{dt} = n_i^P \left( r_i^P - \sum_{j=1}^{S_P} \beta_{ij}^P n_j^P + \dfrac{\sum_{j=1}^{S_A} \gamma_{ij}^P n_j^A}{1 + h_i^P \sum_{j=1}^{S_A} \gamma_{ij}^P n_j^A} \right)
\end{cases} ,
\tag{S89}
$$

where $S_A$ ($S_P$) is the number of animals (plants), and $n_i^A$ ($n_i^P$) is the abundance of animal (plant) species $i$. For the purposes of this section we consider the case of linear functional responses $h_i^A = h_i^P = 0$, as all the methodology used in [14] was developed in this case. If the functional response is linear, this equation reduces to equation S1, where the interaction matrix $\mathbf{A}$ is given by

$$
\mathbf{A} = \begin{pmatrix} -\beta^A & \gamma^A \\ \gamma^P & -\beta^P \end{pmatrix} .
\tag{S90}
$$

Here $\beta^A$ and $\beta^P$ are $S_A \times S_A$ and $S_P \times S_P$ matrices, respectively, while $\gamma^A$ and $\gamma^P$ are $S_A \times S_P$ and $S_P \times S_A$ matrices. The Authors used a constant parameterization for the competition parameters, setting $\beta_{ii}^A = \beta_{ii}^P = 1$ and

$\beta_{ij}^A = \beta_{ij}^P = \rho$ if $j \neq i$. The mutualistic benefits were parameterized as

$$
\begin{aligned}
\gamma_{ij}^A &= \gamma_0 \frac{L_{ij}}{(k_i^A)^\delta} \\
\gamma_{ij}^P &= \gamma_0 \frac{L_{ji}}{(k_i^P)^\delta}
\end{aligned}
, \tag{S91}
$$

where $L_{ij}$ is the nonzero block of the adjacency matrix of the interaction network, i.e., $L_{ij} = 1$ if there is an interaction between animal $i$ and plant $j$, and zero otherwise. The numbers $k_i^A = \sum_{j=1}^{S_P} L_{ij}$ and $k_i^P = \sum_{j=1}^{S_A} L_{ji}$ are the degree of animal/plant $i$. The two remaining parameters, $\gamma_0$ and $\delta$, quantify the levels of mutualistic strength and the mutualistic tradeoff [50].

The method proposed by Rohr et al. [14] was based on what the Authors called the "structural vector". It was defined as the center of feasibility domain and was calculated by transforming the mutualistic dynamics into an effective competitive one. Using this effective dynamics it was possible to calculate an effective structural vector, which was then transformed back to the one of the mutualistic system. Starting from the structural vector, the Authors considered different perturbations of the growth rates by changing their direction from that of the original structural vector by some given angle. The dynamics was then integrated and the probability that all species survived was calculated, given a particular perturbation. Running this across several different perturbations and parameterizations, it was possible to perform a regression between the interaction parameters, the angle by which the growth rates were perturbed, nestedness, and other parameters appearing in the interaction matrix. Using the coefficients obtained through the regression, it was quantified the effect of nestedness and other properties on the size of the feasibility domain.

Here we present some possible issues emerging from this approach. We have not investigated which one of them accounts for the differences we observe. Some of these issues could be relevant, while others could be practically irrelevant for the purpose they were introduced for.

**It is not always possible to find the structural vector**. In order to calculate the structural vector, one needs to transform the mutualistic system into an effective competitive one. One can define the matrix $\mathbf{T} = \mathbf{1} + \gamma\beta^{-1}$, where $\mathbf{1}$ is the identity matrix and

$$
\beta = \begin{pmatrix} \beta^A & 0 \\ 0 & \beta^P \end{pmatrix}, \tag{S92}
$$

and

$$
\gamma = \begin{pmatrix} 0 & \gamma^A \\ \gamma^P & 0 \end{pmatrix}. \tag{S93}
$$

By multiplying both sides of equation S90 by $\mathbf{T}$ one obtains the effective interaction matrix

$$
\mathbf{A}^{\text{eff}} = \begin{pmatrix} -\beta^A + \gamma^P(\beta^\mathbf{P})^{-1}\gamma^A & 0 \\ 0 & -\beta^P + \gamma^A(\beta^\mathbf{A})^{-1}\gamma^P \end{pmatrix} =: \begin{pmatrix} \mathbf{B}_{eff}^A & 0 \\ 0 & \mathbf{B}_{eff}^P \end{pmatrix}, \tag{S94}
$$

In order to calculate the structural vectors, one has to assume that the eigenvectors associated with the largest singular eigenvalues of $(\mathbf{B}_{eff}^A)^t\mathbf{B}_{eff}^A$ and $\mathbf{B}_{eff}^A(\mathbf{B}_{eff}^A)^t$ have only positive components (and an equivalent condition on $\mathbf{B}_{eff}^P$). This is not generally true, as also stated by the Authors [14]. They therefore imposed the extra assumption that $(\mathbf{B}_{eff}^A)^t\mathbf{B}_{eff}^A$ and $\mathbf{B}_{eff}^A(\mathbf{B}_{eff}^A)^t$ indeed have only positive entries (and the equivalent conditions on $\mathbf{B}_{eff}^P$). In this case, the Perron–Frobenius theorem allows all entries of the leading eigenvector to be chosen positive; i.e., it necessarily points in some feasible direction. The Authors then identified the structural vectors with these eigenvectors.

However, the extra requirement that $(\mathbf{B}_{eff}^A)^t\mathbf{B}_{eff}^A$ and $\mathbf{B}_{eff}^A(\mathbf{B}_{eff}^A)^t$ be strictly positive imposes constraints on the interaction matrix that reduces the number of parameterizations that can be analyzed with this method. Since this assumption does not hold in general, there are cases in which the structural vector does not exist. Using our approach, this vector is not needed (see sections S4 and S9).

**When the structural vector exists, it is not unique**. Under what conditions would the matrices $(\mathbf{A}^{\mathrm{eff}})^t\mathbf{A}^{\mathrm{eff}}$ and $\mathbf{A}^{\mathrm{eff}}(\mathbf{A}^{\mathrm{eff}})^t$ respect the condition of Perron–Frobenius theorem? It is easy to show that this can never be the case. From equation S94 we see that $\mathbf{A}^{\mathrm{eff}}$ is block-diagonal, therefore $(\mathbf{A}^{\mathrm{eff}})^t\mathbf{A}^{\mathrm{eff}}$ and $\mathbf{A}^{\mathrm{eff}}(\mathbf{A}^{\mathrm{eff}})^t$ are block-diagonal as well. This means that the Perron–Frobenius theorem does not hold (the matrix is reducible); instead, the two diagonal blocks each have an all-positive leading eigenvector (assuming that all the coefficients are positive in the two blocks). Any linear combination of the two will have positive components (without being an eigenvector). There is no reason to prefer one linear combination over another, and while it is true that some linear combinations may point closer to the center of the feasibility domain, there is no way to determine using the Authors' methods which combination does, if any.

**The structural vector is not the center of the feasibility domain**. Let us assume now that the structural vector exists and it points toward the center of the feasibility domain of the effective competitive system. To obtain the structural vector, one has to transform it back to a vector of the original, mutualistic system. The transformation from the effective to the original system is done by multiplying with the matrix $\mathbf{T}^{-1}$. This matrix is not a rotation, and therefore it does not preserve the angles between vectors. Even if a vector is the center of the feasibility domain in the effective system, it will not in general be the center of the original domain. In particular, its distance to the actual center of the original domain will be dependent on parameterization and network structure, as the transformation matrix depends on these.

In contrast, the center of the feasibility domain can be easily expressed with our approach in terms of the matrix $\mathbf{A}$ (section S3, equation S21). It is also easy to check that the barycenter is different from the one obtained using the method of Rohr et al. [14].

**The regression procedure can in principle produce biases**. The relationship between network structure and the size of the feasibility domain was obtained by calculating the probability of coexistence $p(\theta_A, \theta_P)$, where $\theta_{A/P}$ is the angle by which the direction of the growth rate vector of animals/plants was changed with respect to the

structural vector. The Authors then performed a linear regression

$$\text{logit}(p(\theta_A, \theta_P)) \sim \beta_1 \log \theta_A + \beta_2 \log \theta_B + \beta_3 \gamma_0 C + \beta_4 \gamma_0^2 C^2 + \beta_5 \gamma_0 CN + \beta_6 \gamma_0 CN^2 + \beta_7 \gamma_0 C\delta + \beta_8 \gamma_0 C\delta^2 \quad \text{(S95)}$$

where $C$ is the connectance of the mutualistic adjacency matrix and $N$ is its nestedness (note that $\bar{\gamma}$, used in [14] is equal to $C\gamma_0$). The fitted parameters where then used to determine the effect of nestedness and other quantities on the feasibility domain. The functional dependence assumed above cannot be justified a priori, and an incorrect functional dependence can in principle lead to erroneous fitting results. For instance, the effect of those properties could be different depending not just on the raw angle of perturbation, but also which direction that angle is taken in. We can imagine two feasibility regions with the exact same size but different shapes: one of the two is equally wide in all directions, while the other stretches very wide in some directions but is extremely narrow in others (see section S9). For sufficiently small values of $\theta_{A/P}$, one will never leave the feasible domain in the first of these examples, but may do so in the second if the perturbation is performed in one of the "narrow" directions. The first of these cases will therefore appear more feasible than the second, even though the total size of the two feasibility regions is in fact the same. On the other hand, if the values of $\theta_{A/P}$ are large enough, than the perturbed vector in the first case will never be feasible, while it will be feasible in the second case because of the "wide" directions. Moreover, this method does not allow one to calculate the feasibility domain for a given network and parameterization, as one can calculate only the probability of coexistence given an angle of perturbation.

## S9. DISTRIBUTION OF SIDE LENGTHS

In section S3 we showed that the feasibility domain is a convex polyhedral cone in the space of intrinsic growth rates $\mathbf{r}$. Since the stationary solution of equation S1 is linear in $\mathbf{r}$, we can study the feasibility domain considering only vectors on the unit sphere's surface. In section S4 we defined $\Xi$, which quantifies the volume of the feasibility domain.

The size of the feasibility domain, i.e., how many combinations of the intrinsic growth rates correspond to a feasible fixed point, is not the only interesting property. Two systems having the same number of feasible combinations of growth rates (i.e., the same value of $\Xi$), can respond very differently to perturbations of the growth rates. We imagine here that a perturbation (e.g., a change of the abiotic conditions) correspond to a change in the growth rate vector. Since we can consider normalized growth rate vectors (because of the linearity of the equations), the effect of a perturbation on feasibility depends only on the angular change of the growth rate vector and not on its length.

The volume $\Xi$ quantifies how many growth rate vectors are compatible with coexistence. Let us consider a feasible growth rate vector, and perturb it in a random direction. What is the probability that the new vector is still feasible? This is not just a function of the size of the feasibility domain $\Xi$. Indeed, one can imagine that the feasibility domain is about equally spread in every direction—or that, for the exact same value of $\Xi$, the feasibility domain is streched

in some directions but is very narrow in some other ones. A perturbation in one of the "narrow" directions is much more likely to lead out of the feasibility domain in the latter case than in the former.

To quantify this property, one strategy could be to measure the different responses on the perturbation (i.e., the probability of being feasible) depending on the direction of the perturbation (in which direction we change the growth rate vector). This choice has the big disadvantage of depending not only on the properties of interactions (the interaction matrix $\mathbf{A}$), but also on the strength of the perturbation (the angular displacement between the initial and the final growth rate vector) and the growth rate vector before the perturbation (e.g., if the initial vector is close or far from the edge of the feasibility domain). We propose instead a purely geometrical method to quantify the response to different perturbations (see figure 1 of the main text).

The feasibility domain, when restricted to the surface of a hypersphere, can be imagined as the generalization of a triangle on a sphere (see section S11). The natural, geometric quantities bounding the maximal perturbation that will leave the system feasible, are the lengths of the triangle's sides. When $S$ species are considered, there are $S(S-1)/2$ sides. Their lengths measure the maximum permissible perturbation of the growth rates in the corresponding direction if one is to retain feasibility. This property has the advantage of being purely geometrical, depending only on the interactions (via the interaction matrix) and not, for instance, on any choice of the initial conditions.

We can measure the distribution of the side lengths. Imagine we have two interaction matrices with the same $\Xi$, but with very different distributions of side lengths. One of them has all sides of equal length, while the other one has a more heterogeneous distribution. In the first case any direction of the perturbation is expected to have a similar effect, and there are no particularly dangerous directions. In the second case there are some directions of the perturbation that are much more dangerous than others, and even a small change of conditions along one of those dangerous direction can lead to the extinction of one or more species.

### A. Defining side lengths

We know that the feasibility domain is a convex polyhedral cone (see section S3). Its "corners" are identified by its generators and its sides are determined by all pairs of generators (see section S11 for the $S = 3$ case).

Since we are considering growth rates on the unit (hyper)sphere, and the generators are normalized to one, any pair of generators will lie on the sphere's surface. The scalar product of two generators is the cosine of the angle between the two. Since the two generators are on the unit ball's surface, the arc between the two (which is the side length) is equal to the angle. We have therefore that the length of the side of the feasibility domain corresponding to a pair of generators $\mathbf{g}^i$ and $\mathbf{g}^j$ is

$$\eta_{ij} = \arccos \left( \mathbf{g}^i \cdot \mathbf{g}^j \right) \ . \tag{S96}$$

Using equation S12, we can express the $S(S-1)/2$ side lengths of the convex polytope explicitly in terms of the

interaction matrix:

$$\eta_{ij} = \arccos\left(\frac{\sum_k A_{ki} A_{kj}}{\sqrt{\sum_k A_{ki} A_{ki} \sum_l A_{lj} A_{lj}}}\right) . \tag{S97}$$

We are interested in the distribution of the side lengths, and in particular in its heterogeneity. In the following section we will calculate these quantities for random matrices.

## B.    The distribution of side lengths in random matrices

In this section we obtain the distribution of sides length for large random matrices, whose entries are distributed accordingly to an arbitrarily bivariate distribution.

We assume that the diagonal elements of $\mathbf{A}$ are all equal to $-d$ (this hypothesis can be easily generalized), while the offdiagonal pairs $(A_{ij}, A_{ji})$ are random variables with distribution $q(x, y)$. Our goal is to find the distribution of the side lengths $\eta$ in the large $S$ limit, defined as

$$\begin{aligned}
P(\eta) = \lim_{S \to \infty} \frac{1}{S(S-1)} \sum_{i \neq j} \int \prod_{m>n} \Big( \mathrm{d}A_{mn} \mathrm{d}A_{nm} q(A_{mn}, A_{nm}) \Big) \\
\times \delta\left( \eta - \arccos\left( \frac{\sum_k A_{ki} A_{kj}}{\sqrt{\sum_k A_{ki} A_{ki} \sum_l A_{lj} A_{lj}}} \right) \right),
\end{aligned} \tag{S98}$$

Since we are summing over all $i$ and $j$, and all the rows are identically distributed, we can remove the sum and consider just two rows:

$$\begin{aligned}
P(\eta) = \lim_{S \to \infty} \int \prod_{m>n} \Big( \mathrm{d}A_{mn} \mathrm{d}A_{nm} q(A_{mn}, A_{nm}) \Big) \\
\times \delta\left( \eta - \arccos\left( \frac{\sum_k A_{k1} A_{k2}}{\sqrt{\sum_k A_{k1} A_{k1} \sum_l A_{l2} A_{l2}}} \right) \right),
\end{aligned} \tag{S99}$$

Since we are interested in the large $S$ limit, we have that

$$\begin{aligned}
\sum_k A_{k1} A_{k1} =& A_{11} + \sum_{k>1} (A_{k1})^2 \approx -d + (S-1) \int \mathrm{d}x \mathrm{d}y \, q(x, y) \, x^2 \\
=& -d + (S-1)(E_1^2 + E_2^2),
\end{aligned} \tag{S100}$$

where $E_1$ and $E_2$ are the first and second marginal moments of $q$ (equations S36 and S37). Let us call this quantity

$Z$. In this limit we therefore obtain

$$
\begin{aligned}
P(\eta) &= \lim_{S\to\infty} \int \prod_{m>n} \left( \mathrm{d}A_{mn}\mathrm{d}A_{nm}q(A_{mn}, A_{nm}) \right) \delta\left( \eta - \arccos\left( \frac{\sum_k A_{k1}A_{k2}}{Z} \right) \right) \\
&= \lim_{S\to\infty} \int \prod_{m>n} \left( \mathrm{d}A_{mn}\mathrm{d}A_{nm}q(A_{mn}, A_{nm}) \right) Z \, |\sin(\eta)| \, \delta\left( Z\cos(\eta) - \sum_k A_{k1}A_{k2} \right) \\
&= Z|\sin(\eta)| \lim_{S\to\infty} \int \prod_{m>n} \left( \mathrm{d}A_{mn}\mathrm{d}A_{nm}q(A_{mn}, A_{nm}) \right) \delta\left( Z\cos(\eta) - \sum_k A_{k1}A_{k2} \right) \\
&= Z|\sin(\eta)| \lim_{S\to\infty} \int \prod_{m>n} \left( \mathrm{d}A_{mn}\mathrm{d}A_{nm}q(A_{mn}, A_{nm}) \right) \\
&\quad \times \delta\left( Z\cos(\eta) - A_{11}A_{21} - A_{22}A_{12} - \sum_{k>2} A_{k1}A_{k2} \right) \\
&= Z|\sin(\eta)| \lim_{S\to\infty} \int \prod_{m>n} \left( \mathrm{d}A_{mn}\mathrm{d}A_{nm}q(A_{mn}, A_{nm}) \right) \\
&\quad \times \delta\left( Z\cos(\eta) + d(A_{12} + A_{21}) - \sum_{k>2} A_{k1}A_{k2} \right) \\
&= Z|\sin(\eta)| \int \mathrm{d}t \int \mathrm{d}s \int \mathrm{d}A_{12}\mathrm{d}A_{21}q(A_{12}, A_{21})\delta(t - A_{12} - A_{21}) \\
&\quad \times \int \prod_{k>2} \mathrm{d}A_{k1}\mathrm{d}A_{k2}q(A_{k1})q(A_{k2})\delta\left( s - \sum_{k>2} A_{k1}A_{k2} \right) \\
&\quad \times \delta\left( Z\cos(\eta) + dt - \sum_{k>2} A_{k1}A_{k2} \right) \\
&= Z|\sin(\eta)| \int \mathrm{d}t \int \mathrm{d}s \int \mathrm{d}x\mathrm{d}y \, q(x,y)\delta(t - (x+y)) \\
&\quad \times \int \left( \prod_{k=1}^{S-2} dz_k dw_k q(z_k)q(w_k) \right) \delta\left( s - \sum_{k=1}^{S-2} z_k w_k \right) \delta(Z\cos(\eta) + dt - s) \,,
\end{aligned}
\tag{S101}
$$

where $q(z)$ is the marginal distribution of $q(x,y)$:

$$
q(z) = \int \mathrm{d}x \, q(x,z) = \int \mathrm{d}x \, q(z,x).
\tag{S102}
$$

We can introduce the distribution of the sum:

$$
q_s(t) = \int \mathrm{d}x\mathrm{d}y q(x,y)\delta(t - (x+y)).
\tag{S103}
$$

The term

$$
\int \left( \prod_{k=1}^{S-2} dz_k dw_k \, q(z_k)q(w_k) \right) \delta\left( s - \sum_{k=1}^{S-2} z_k w_k \right)
\tag{S104}
$$

is the distribution of a sum of $S-2$ uncorrelated random variables. These random variables are the product $zw$ of two random variables whose distribution is $q$. Since the second moment of $q(x)$ is finite, the central limit theorem holds and this distribution converges, in the large $S$ limit, to a Gaussian distribution with mean

$$
S \int \mathrm{d}x\mathrm{d}y \, q(y)q(x) \, xy = SE_1^2
\tag{S105}
$$

and variance

$$S\left(\int \mathrm{d}x\mathrm{d}y \; q(y)q(x) \; (xy)^2 - E_1^2\right) = SE_2^4 \; . \tag{S106}$$

We have therefore

$$P(\eta) = Z|\sin(\eta)| \int \mathrm{d}t\mathrm{d}s \; q_s(t) \frac{\exp\left(\frac{-(s-SE_1^2)^2}{2SE_2^4}\right)}{\sqrt{2S\pi E_2^2}} \delta(Z\cos(\eta) + dt - s) = (S(E_1^2 + E_2^2) - d)$$

$$\times \frac{|\sin(\eta)|}{\sqrt{2S\pi E_2^2}} \int \mathrm{d}t \; q_s(t) \exp\left(-\frac{\left(S(E_1^2 + E_2^2)\cos(\eta) - d\cos(\eta) - SE_1^2 + dt\right)^2}{2SE_2^4}\right) \; . \tag{S107}$$

The distribution of $\eta$ is not universal as it depends on $q_s(t)$, which depends on the distribution of the coefficients. On

the other hand, the dependence is explicit, and it is possible to calculate $P(\eta)$ for any distribution $q(x, y)$.

We show explicitly the case of $q(x, y)$ being a bivariate normal distribution, i.e.,

$$q(x, y) = \frac{1}{2\pi E_2^2 \sqrt{1 - E_c^2}} \exp\left(-\frac{(x - E_1)^2 + (y - E_1)^2 - 2E_c(x - E_1)(y - E_1)}{2E_2^2}\right) \; . \tag{S108}$$

In this case $q_s(t)$ is a normal distribution, and can be obtained from eq S103

$$q_s(t) = \frac{1}{2\pi E_2^2 \sqrt{1 - E_c^2}} \int \mathrm{d}y \exp\left(-\frac{(t - y - E_1)^2 + (y - E_1)^2 - 2E_c(t - y - E_1)(y - E_1)}{2E_2^2}\right)$$

$$= \exp\left(-\frac{(1 - E_c)(t - 2E_1)^2}{4E_2^2}\right) \frac{1}{2\sqrt{\pi}E_2(1 + E_c)\sqrt{1 - E_c}} \; . \tag{S109}$$

Substituting into equation S107, we see that $P(\eta)$ has the form of a convolution of two Gaussians, and turns out to

be equal to

$$P(\eta) = \frac{|\sin(\eta)|}{\sqrt{2\pi}\,\mathrm{var}(\cos(\eta))} \exp\left(-\frac{\big(\cos(\eta) - \langle\cos(\eta)\rangle\big)^2}{2\,\mathrm{var}(\cos(\eta))}\right) \; . \tag{S110}$$

The mean $\langle\cos(\eta)\rangle$ and variance $\mathrm{var}(\cos(\eta))$ will be computed in the next section in the most general case of an

arbitrary interaction distribution.

## C. Moments for random matrices

As explained in the previous section, the distribution of the side lengths is not a universal quantity, as it depends

on the distribution of interaction strengths. In this section we compute the mean and the variance in the general case,

showing that they depends only on $E_1$, $E_2$ and $E_c$.

Here and in the main text we do not report the moments of the side length $\eta$, but the moments of its cosine. The

cosine of the side length measures the overlap between two rows of the interaction matrix (or the scalar product of

two generators of the convex polytope). As its value gets close to one, the side length approaches zero.

Starting from equation S97, we have that

$$\big\langle \cos(\eta) \big\rangle = \frac{1}{S(S-1)} \sum_{i\neq j} \cos(\eta_{ij}) = \frac{1}{S(S-1)} \sum_{i\neq j} \left(\frac{\sum_k A_{ik}A_{jk}}{\sqrt{\sum_k A_{ik}A_{ik}\sum_l A_{jl}A_{jl}}}\right) , \tag{S111}$$

Since we are interested in the large $S$ limit, we can write the denominator as in equation S100 and obtain

$$\langle \cos(\eta) \rangle = \frac{1}{S(S-1)} \sum_{i \neq j} \left( \frac{\sum_k A_{ik} A_{jk}}{-d + S(E_1^2 + E_2^2)} \right) \ , \tag{S112}$$

and then

$$\langle \cos(\eta) \rangle = \frac{1}{S(S-1)} \sum_{i \neq j} \left( \frac{A_{ii} A_{ji} + A_{ij} A_{jj} + \sum_{k \neq i,j} A_{ik} A_{jk}}{-d + S(E_1^2 + E_2^2)} \right) \ . \tag{S113}$$

In the large $S$ limit, this becomes

$$\langle \cos(\eta) \rangle = \frac{-2dE_1 + SE_1^2}{-d + (S-2)(E_1^2 + E_2^2)} \tag{S114}$$

to leading order in $S$.

In a similar way, we can write the second moment as

$$\langle \cos(\eta)^2 \rangle = \frac{1}{S(S-1)} \sum_{i \neq j} \cos(\eta_{ij})^2 = \frac{1}{S(S-1)} \sum_{i \neq j} \left( \frac{\sum_k A_{ik} A_{jk}}{\sqrt{\sum_k A_{ik} A_{ik} \sum_l A_{jl} A_{jl}}} \right)^2 \ . \tag{S115}$$

In the large $S$ limit we obtain

$$\begin{aligned}
\langle \cos(\eta)^2 \rangle &= \frac{1}{S(S-1)} \sum_{i \neq j} \frac{\left( \sum_k A_{ik} A_{jk} \right)^2}{\left( -d + S(E_1^2 + E_2^2) \right)^2} = \frac{1}{S(S-1)} \sum_{i \neq j} \frac{\sum_k \sum_l A_{ik} A_{jk} A_{il} A_{jl}}{\left( -d + S(E_1^2 + E_2^2) \right)^2} \\
&= \frac{1}{S(S-1)} \sum_{i \neq j} \frac{\left( A_{ii} A_{ji} + A_{ij} A_{jj} + \sum_{k \neq i,j} A_{ik} A_{jk} \right) \left( A_{ii} A_{ji} + A_{ij} A_{jj} + \sum_{l \neq i,j} A_{il} A_{jl} \right)}{\left( -d + S(E_1^2 + E_2^2) \right)^2} \\
&= \frac{1}{S(S-1)} \sum_{i \neq j} \frac{d^2 (A_{ij} + A_{ji})^2 - 2d(A_{ij} + A_{ji}) \sum_{k \neq i,j} A_{ik} A_{jk} + (\sum_{k \neq i,j} A_{ik} A_{jk})^2}{\left( -d + S(E_1^2 + E_2^2) \right)^2} \ .
\end{aligned} \tag{S116}$$

We can compute the averages of the different terms, obtaining

$$\begin{aligned}
\frac{1}{S(S-1)} \sum_{i \neq j} (A_{ij} + A_{ji})^2 &= \frac{1}{S(S-1)} \sum_{i \neq j} (A_{ij}^2 + A_{ji}^2 + 2A_{ji} A_{ij}) \\
&= 2(E_1^2 + E_2^2) + 2(E_c E_2^2 + E_1^2) = 4E_1^2 + 2(1 + E_c) E_2^2 \ ,
\end{aligned} \tag{S117}$$

$$\begin{aligned}
\frac{1}{S(S-1)} \sum_{i \neq j} (A_{ij} + A_{ji}) \sum_{k \neq i \neq j} A_{ik} A_{jk} &= \frac{1}{S(S-1)} \sum_{i \neq j} (A_{ij} + A_{ji})(S-2) E_1^2 \\
&= 2(S-2) E_1^3 \ ,
\end{aligned} \tag{S118}$$

and

$$\begin{aligned}
\frac{1}{S(S-1)} \sum_{i \neq j} \left( \sum_{k \neq i \neq j} A_{ik} A_{jk} \right)^2 &= \frac{1}{S(S-1)} \sum_{i \neq j} \sum_{k \neq i,j} \sum_{l \neq i,j} A_{ik} A_{il} A_{jk} A_{jl} \\
&= \frac{1}{S(S-1)} \sum_{i \neq j} \sum_{k \neq i,j} \left( \sum_{l \neq i,j,k} (A_{ik} A_{il} A_{jk} A_{jl}) + A_{ik}^2 A_{jk}^2 \right) \\
&= (S-2)(S-3) E_1^4 + (S-2)(E_1^2 + E_2^2)^2 \ .
\end{aligned} \tag{S119}$$

We finally get that, in the large $S$ limit,

$$\mathrm{var}(\cos(\eta)) = \left\langle \cos(\eta)^2 \right\rangle - \left\langle \cos(\eta) \right\rangle^2 = \frac{2d^2(1 + E_c)E_2^2 + S(E_2^2 + E_1^2)^2 - SE_1^4}{(-d + S(E_1^2 + E_2^2))^2} \ . \tag{S120}$$

## S10. SIDE HETEROGENEITY FOR DIFFERENT STRUCTURES AND EMPIRICAL NETWORKS

In the main text we considered the effect of four nonrandom structures on the mean and variance of the side lengths. Here we explain how those interaction matrices were constructed. To generate figure 3 of the main text, we always considered a connectance of $C = 0.2$. The interaction strengths were drawn from a normal distribution with given mean, variance, and correlation. For some structures we considered multiple interaction types and therefore multiple means (one positive and one negative), in which case the coefficient of variation of the interactions and the correlation was constant and independent of the mean.

- **Modular**. In this case we considered interaction matrices with a perfect block structure (to generate figure 3 we considered four blocks of equal size).

- **Bipartite**. In this case we considered an interaction matrix with two bipartite blocks of equal size. The mean interaction of the offdiagonal blocks was set to be negative, while the one of the in-diagonal blocks was positive.

- **Nested**. The interaction matrix had a bipartite structure. The diagonal blocks had a random structure with negative mean interaction strength. In the offdiagonal blocks, we consider a connectance equal to one half and we built a perfectly nested matrix. The mean interaction strength was positive in the offdiagonal blocks.

- **Cascade**. We build a matrix using the cascade model, and parameterize it with a positive and a negative mean depending on the role of the species in the interaction.

We considered the same networks and the same parameterization explained in section S7. We compared $\left\langle \cos(\eta) \right\rangle$ and $\mathrm{var}(\cos(\eta))$ with the values expected in the random case.

## S11. FEASIBILITY DOMAIN FOR $S = 3$

When $S = 3$, it is possible to visualize in three dimensions a convex polyhedral cone and the feasibility domain. In figure S4 we show a convex polyhedral cone in three dimensions and its generators.

An important feature of convex polyhedral cones is that if $\mathbf{r}$ belongs to the cone, then so does $c\mathbf{r}$ for any positive constant $c$. As explained in section S3, this is a consequence of the linearity of equation S1. It is relevant therefore to limit our analysis to the growth rate vectors on the unit sphere, i.e., to vectors $\mathbf{r}$ such that

$$\|\mathbf{r}\| = \sqrt{r_1^2 + r_2^2 + r_3^2} = 1 \ . \tag{S121}$$
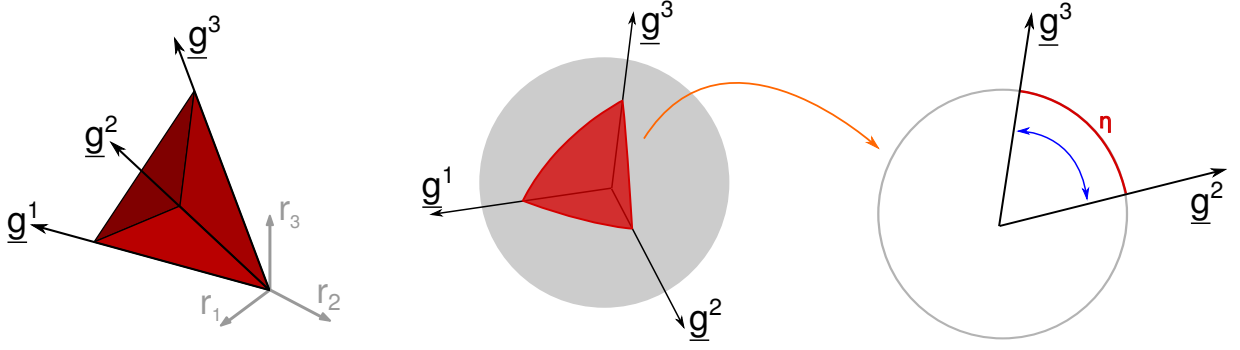
Supplementary Figure S4: Convex polyhedral cone and its section on a sphere. Left: the feasibility domain is a convex polyhedral cone, which is completely determined by its $S$ generators (when $S = 3$ we have 3 generators $\mathbf{g}^1$, $\mathbf{g}^2$, and $\mathbf{g}^3$). Center: since we consider a linear equation we can focus the analysis only on the intersection between the convex polyhedral cone and the unit sphere's surface, which in three dimensions results in a spherical triangle. Right: each side of the convex polyhedral cone can be determined from a pair of generators as an arc $\eta$ of the sphere's surface. Since we are considering the unit sphere, the arc length $\eta$ is equal to the angle between the two generators.

When we consider the vector in the feasibility domain on the surface of a unit sphere we obtain the areas of figure 1 in the main text. In this case, the quantity $\Xi$ is the area of the triangle, while the side lengths are the three sides of the triangle. Note that the polygon is not a triangle (as it lies on a sphere), but rather a spherical triangle. Its sides are arcs of a circumference, while its corners are identified by the three generators of the convex polyhedral cone.

In the $S = 3$ case it is possible to obtain a closed expression for the area $\Xi$ [30]:

$$\Xi = \frac{8}{\pi} \arctan\left(\frac{|\det(\mathbf{G})|}{1 + \mathbf{g}^1 \cdot \mathbf{g}^2 + \mathbf{g}^2 \cdot \mathbf{g}^3 + \mathbf{g}^1 \cdot \mathbf{g}^3}\right) + \Theta\left(-1 - \mathbf{g}^1 \cdot \mathbf{g}^2 - \mathbf{g}^2 \cdot \mathbf{g}^3 - \mathbf{g}^1 \cdot \mathbf{g}^3\right) , \tag{S122}$$

where the second term adds one to the first term when the argument of the arctangent is negative, while the matrix $\mathbf{G}$ is defined as

$$G_{ij} = \mathbf{g}^i \cdot \mathbf{g}^j . \tag{S123}$$

Equation S122 can be expressed directly in terms of the matrix $\mathbf{A}$ using equation S12.

## S12.  NON-LINEAR FUNCTIONAL RESPONSES

In general, the effect of a species on per-capita growth rates of one other species is not linear. Equation S1 assumes this response to be linear and the results presented in this paper were obtained under this assumption. Non-linearity in the functional response can be tough as a dependence of the interaction matrix $\mathbf{A}$ on $\mathbf{n}$

$$\frac{\mathrm{d}n_i}{\mathrm{d}t} = n_i \left( r_i + \sum_{j=1}^{S} A_{ij}(\mathbf{n}) n_j \right) . \tag{S124}$$

For instance, in the case of a Holling type II functional response, it would have the form

$$A_{ij}(\mathbf{n}) = \frac{A_{ij}^0}{1 + \sum_j h_{ij} A_{ij}^0 n_j} \ , \tag{S125}$$

where $h_{ij}$ are known as handling times.

The presence of a non linearity has a strong effect on both feasibility and stability. First of all it is not possible to disentangle feasibility from stability with a simple condition on $A_{ij}^0$. Then feasibility depends in this case not only on the direction of $\mathbf{r}$, but also on its norm.

The results presented here are the necessary step to include non linearity in functional responses. When the degree of non-linearity is small enough (e.g., $h_{ij} \approx 0$), one can use our result (valid in the case $h_{ij} = 0$) to find the center of the feasibility domain and the generating vectors. One can use their position to estimate the volume of the feasibility domain in the case $h_{ij} > 0$. Since on expect it to be not too different from the $h_{ij} = 0$, it is possible to numerically explore only the region around the generators and estimate in this way the feasibility domain.

It is possible to show, that in the limit of very large $h$, the non linear functional response in approximately linear and it is possible to use again our method. Since it applies both in the case of small and large values of $h$, we expect that the presence of an intermediate value of $h$ does not affect drastically the result.

[1] J F Gillooly, J H Brown, G B West, V M Savage, and E L Charnov. Effects of size and temperature on metabolic rate. Science (New York, N.Y.), 293(5538):2248–51, October 2001.

[2] Gian-Reto Walther, Eric Post, Peter Convey, Annette Menzel, Camille Parmesan, Trevor J C Beebee, Jean-Marc Fromentin, Ove Hoegh-Guldberg, and Franz Bairlein. Ecological responses to recent climate change. Nature, 416(6879):389–95, March 2002.

[3] Jason M. Tylianakis, Raphael K. Didham, Jordi Bascompte, and David A. Wardle. Global change and species interactions in terrestrial ecosystems. Ecology Letters, 11(12):1351–1363, December 2008.

[4] Jason P Harmon, Nancy A Moran, and Anthony R Ives. Species response to environmental change: impacts of food web interactions and evolution. Science (New York, N.Y.), 323(5919):1347–50, March 2009.

[5] Jason M. Tylianakis, Etienne Laliberté, Anders Nielsen, and Jordi Bascompte. Conservation of species interaction networks. Biological Conservation, 143(10):2270–2279, October 2010.

[6] V.I. Arnold. Geometrical Methods in the Theory of Ordinary Differential Equations. Springer, 2012.

[7] Robert M. May and Warren J. Leonard. Nonlinear Aspects of Competition Between Three Species. SIAM Journal on Applied Mathematics, 29(2):243–253, September 1975.

[8] Robert M May. Will a Large Complex System be Stable? Nature, 238(5364):413–414, August 1972.

[9] Stefano Allesina and Si Tang. Stability criteria for complex ecosystems. Nature, February 2012.

[10] Samir Suweis, Jacopo Grilli, and Amos Maritan. Disentangling the effect of hybrid interactions and of the constant effort hypothesis on ecological community stability. Oikos, 123(5):525–532, May 2014.

[11] Michael E. Gilpin. Stability of feasible predator-prey systems. Nature, 254(5496):137–139, March 1975.

[12] Alan Roberts. The stability of a feasible random ecosystem. Nature, 251(5476):607–608, October 1974.

[13] B.S. Goh and L.S. Jennings. Feasibility and stability in randomly assembled Lotka-Volterra models. Ecological Modelling, 3(1):63–71, February 1977.

[14] R. P. Rohr, S. Saavedra, and Jordi Bascompte. On the structural stability of mutualistic systems. Science, 345(6195):1253497–1253497, July 2014.

[15] Si Tang and Stefano Allesina. Reactivity and stability of large ecosystems. Frontiers in Ecology and Evolution, 2, June 2014.

[16] Serguei Saavedra, Rudolf P Rohr, Luis J Gilarranz, and Jordi Bascompte. How structurally stable are global socioeconomic systems? Journal of the Royal Society, Interface / the Royal Society, 11(100):20140693, November 2014.

[17] Stefano Allesina and Si Tang. The stabilitycomplexity relationship at age 40: a random matrix perspective. Population Ecology, 57(1):63–75, January 2015.

[18] J E Cohen, F Briand, and C M Newman. Community food webs: Data and theory. Springer-Verlag, Berlin, 1990.

[19] R J Williams and N D Martinez. Simple rules yield complex food webs. Nature, 404(6774):180–3, March 2000.

[20] Jordi Bascompte, Pedro Jordano, Carlos J Melián, and Jens M Olesen. The nested assembly of plant-animal mutualistic networks. Proceedings of the National Academy of Sciences of the United States of America, 100(16):9383–7, August 2003.

[21] Jordi Bascompte, Pedro Jordano, and Jens M Olesen. Asymmetric coevolutionary networks facilitate biodiversity maintenance. Science (New York, N.Y.), 312(5772):431–3, April 2006.

[22] Ugo Bastolla, Miguel A Fortuna, Alberto Pascual-García, Antonio Ferrera, Bartolo Luque, and Jordi Bascompte. The architecture of mutualistic networks minimizes competition and increases biodiversity. Nature, 458(7241):1018–20, April 2009.

[23] Elisa Thébault and Colin Fontaine. Stability of ecological communities and the architecture of mutualistic and trophic networks. Science (New York, N.Y.), 329(5993):853–6, August 2010.

[24] Samir Suweis, Filippo Simini, Jayanth R Banavar, and Amos Maritan. Emergence of structural and dynamical properties of ecological mutualistic networks. Nature, 500(7463):449–52, August 2013.

[25] Alex James, Jonathan W Pitchford, and Michael J Plank. Disentangling nestedness from models of ecological complexity. Nature, 487(7406):227–30, July 2012.

[26] Eugenius Kaszkurewicz and Amit Bhaya. Matrix Diagonal Stability in Systems and Computation. Birkhäuser Boston, Boston, MA, 2000.

[27] Abraham Berman and Daniel Hershkowitz. Matrix diagonal stability and its implications. SIAM Journal on Algebraic Discrete Methods, 4(3):377–382, 1983.

[28] B. S. Goh. Global Stability in Many-Species Systems, 1977.

[29] R. Tyrrell Rockafellar. Convex Analysis. Princeton University Press, 1997.

[30] Daniel Gourion and Alberto Seeger. Deterministic and stochastic methods for computing volumetric moduli of convex cones. Computational & Applied Mathematics, 29(2):215–246, 2010.

[31] Terence Tao, Van Vu, and Manjunath et al. Krishnapur. Random matrices: Universality of ESDs and the circular law. The Annals of Probability, 38(5):2023–2065, September 2010.

[32] Terence Tao and Van Vu. Random Matrices: Universality of Local Eigenvalue Statistics up to the Edge. Communications in Mathematical Physics, 298(2):549–572, April 2010.

[33] Terence Tao and Van Vu. Random matrices: Universality of local eigenvalue statistics. Acta Mathematica, 206(1):127–204, March 2011.

[34] S Allesina and S Tang. The stability-complexity relationship at age 40. {A} {R}andom {M}atrix Perspective. Population Ecology, (accepted), 2014.

[35] Giorgio Parisi. Statistical Field Theory. Perseus Books, 1998.

[36] T. H. Berlin and M. Kac. The Spherical Model of a Ferromagnet. Physical Review, 86(6):821–835, June 1952.

[37] Joel E Cohen, Daniella N Schittler, David G Raffaelli, and Daniel C Reuman. Food webs are more than the sum of their tritrophic parts. Proceedings of the National Academy of Sciences, 106(52):22335–22340, 2009.

[38] Robert R Christian and Joseph J Luczkovich. Organizing and understanding a winter's seagrass foodweb network through effective trophic levels. Ecological Modelling, 117(1):99–124, 1999.

[39] Marie-France Cattin Blandenier. Food web ecology: models and application to conservation. PhD thesis, 2004.

[40] Edward B Baskerville, Andy P Dobson, Trevor Bedford, Stefano Allesina, T Michael Anderson, and Mercedes Pascual. Spatial guilds in the Serengeti food web revealed by a Bayesian group model. PLoS computational biology, 7(12):e1002321, 2011.

[41] C Dieter Zander, Neri Josten, Kim C Detloff, Robert Poulin, John P McLaughlin, and David W Thieltges. Food web including metazoan parasites for a brackish shallow water ecosystem in Germany and Denmark: Ecological Archives E092-174. Ecology, 92(10):2007, 2011.

[42] Kim N Mouritsen, Robert Poulin, John P McLaughlin, and David W Thieltges. Food web including metazoan parasites for an intertidal ecosystem in New Zealand: Ecological Archives E092-173. Ecology, 92(10):2006, 2011.

[43] Neo D Martinez. Artifacts or attributes? Effects of resolution on the Little Rock Lake food web. Ecological Monographs, 61:367–392, 1991.

[44] David W Thieltges, Karsten Reise, Kim N Mouritsen, John P McLaughlin, and Robert Poulin. Food web including metazoan parasites for a tidal basin in Germany and Denmark: Ecological Archives E092-172. Ecology, 92(10):2005, 2011.

[45] Silvia Opitz. Trophic interactions in Caribbean coral reefs. Number 1085. WorldFish, 1996.

[46] Ute Jacob, Aaron Thierry, Ulrich Brose, Wolf E Arntz, Sofia Berg, Thomas Brey, Ingo Fetzer, Tomas Jonsson, Katja Mintenbeck, Christian Mollmann, and Others. The role of body size in complex food webs: A cold case. Advances In Ecological Research, 45:181–223, 2011.

[47] Ryan F Hechinger, Kevin D Lafferty, John P McLaughlin, Brian L Fredensborg, Todd C Huspeni, Julio Lorda, Parwant K Sandhu, Jenny C Shaw, Mark E Torchin, Kathleen L Whitney, and Others. Food webs including parasites, biomass, body sizes, and life stages for three California/Baja California estuaries: Ecological Archives E092-066. Ecology, 92(3):791, 2011.

[48] Jens O Riede, Ulrich Brose, Bo Ebenman, Ute Jacob, Ross Thompson, Colin R Townsend, and Tomas Jonsson. Stepping in {E}lton's footprints: a general scaling model for body masses and trophic levels across ecosystems. Ecology Letters, 14(2):169–178, 2011.

[49] Ute Jacob. Trophic dynamics of Antarctic shelf ecosystems: food webs and energy flow budgets. PhD thesis, Bremen, Univ., Diss., 2005, 2005.

[50] Serguei Saavedra, Rudolf P Rohr, Vasilis Dakos, and Jordi Bascompte. Estimating the tolerance of species to the effects of global environmental change. Nature communications, 4:2350, January 2013.